OFFICE OF NAVAL RESEARCH

Contract N00014-84-K-0021

Technical Report No. 15

Anomalous Behavior of Cured Epoxy Resins: Density at Room Temperature Vs. Time and Temperature of Cure

by

K. P. Pang and J. K. Gillham

To be published in the Journal of Applied Polymer Science

Polymer Materials Program
Department of Chemical Engineering
Princeton University
Princeton, NJ 08544

July 1988

Principal Investigator
John K. Gillham
(609) 452-4694

SECURITY CLASSIFICATION OF THIS PAGE (When Data Entered)

REPORT DOCUMENTATION PAGE		READ INSTRUCTIONS BEFORE COMPLETING FORM
1 REPORT NUMBER: Technical Report #15	2 GOVT ACCESSION NO: N/A	3 RECIPIENT'S CATALOG NUMBER: N/A
4 TITLE (and Subtitle): Anomalous Behavior of Cured Epoxy Resins: Density at Room Temperature Vs. Time and Temperature of Cure		5 TYPE OF REPORT & PERIOD COVERED: 1/7/87 - 1/7/88
		6 PERFORMING ORG. REPORT NUMBER
7 AUTHOR(s): K. P. Pang and J. K. Gillham		8 CONTRACT OR GRANT NUMBER(s): N00014-84-K-0021
9 PERFORMING ORGANIZATION NAME AND ADDRESS: Polymer Materials Program, Department of Chemical Engineering, Princeton University, Princeton, NJ 08544		10 PROGRAM ELEMENT, PROJECT, TASK AREA & WORK UNIT NUMBERS
11 CONTROLLING OFFICE NAME AND ADDRESS: Office of Naval Research, Attn: Code 413, 800 N. Quincy St., Arlington, VA 22217		12 REPORT DATE: July 1988
		13 NUMBER OF PAGES: 48
14 MONITORING AGENCY NAME & ADDRESS (if different from Controlling Office)		15 SECURITY CLASS. (of this report): Unclassified
		15a DECLASSIFICATION/DOWNGRADING SCHEDULE

16 DISTRIBUTION STATEMENT (of this Report)

Approved for public release; distribution unlimited.

17 DISTRIBUTION STATEMENT (of the abstract entered in Block 20, if different from Report)

N/A

18 SUPPLEMENTARY NOTES

19 KEY WORDS (Continue on reverse side if necessary and identify by block number)

Cure, Kinetics, Density, Conversion, Vitrification, Time-Temperature-Transformation Cure Diagram, Glass Transition, Physical Aging

20 ABSTRACT (Continue on reverse side if necessary and identify by block number)

The room temperature density (ρ_{RT}) of a difunctional aromatic epoxy resin cured with a tetrafunctional aromatic amine passes through a maximum value with increasing conversion. For a given cooling rate cure results in a unique value of ρ_{RT} for each conversion as long as the material does not vitrify on cure. The occurrence of vitrification during cure eliminates the one-to-one relationship because of the non-equilibrium nature of the glass transition region and of the glassy state. In the glass transition region there is

DD FORM 1 JAN 73 1473 EDITION OF 1 NOV 65 IS OBSOLETE

S/N 0102-014-6601

SECURITY CLASSIFICATION OF THIS PAGE (When Data Entered)

competition between physical aging which increases the density and chemical aging which decreases ρ_{RT}. Prolonged isothermal cure and physical aging to well beyond vitrification result in limiting values of ρ_{RT} which decrease with increasing temperature of cure. The maximum in ρ_{RT} vs. conversion relationship is discussed in terms of the effects of shrinkage due to cure, the corresponding non-linear increase in the glass transition temperature with increasing conversion, and longer relaxation times in the glass transition region with increasing crosslink density. Other factors which affect room temperature density are discussed.

Resins
D#15

Anomalous Behavior of Cured Epoxy Resins:

Density at Room Temperature vs. Time and Temperature of Cure

K. P. Pang and J. K. Gillham

Polymer Materials Program

Department of Chemical Engineering

Princeton University

Princeton, NJ 08544

ABSTRACT

The room temperature density (ρ_{RT}) of a difunctional aromatic epoxy resin cured with a tetrafunctional aromatic amine passes through a maximum value with increasing conversion. For a given cooling rate cure results in a unique value of ρ_{RT} for each conversion as long as the material does not vitrify on cure. The occurrence of vitrification during cure eliminates the one-to-one relationship because of the non-equilibrium nature of the glass transition region and of the glassy state. In the glass transition region there is competition between physical aging which increases the density and chemical aging which decreases ρ_{RT}. Prolonged isothermal cure and physical aging to well beyond vitrification result in limiting values of ρ_{RT} which decrease with increasing temperature of cure. The maximum in ρ_{RT} vs. conversion relationship is discussed in terms of the effects of shrinkage due to cure, the corresponding non-linear increase in the glass transition temperature with increasing conversion, and longer relaxation times in the glass transition region with increasing crosslink density. Other factors which affect room temperature density are discussed.

INTRODUCTION

Recent studies on the cure and properties of difunctional [1-3] and trifunctional [3] aromatic epoxy resins cured with tetrafunctional aromatic diamines showed that, at room temperature (RT), the shear modulus and density (ρ_{RT}) decreased and the equilibrium level of water absorbed increased with increasing conversion. The common underlying reason for these phenomena in terms of free volume is not at all obvious. In principle, increased extent of cure will increase molecular weight and crosslinking, which remove free ends and restrain thermal motions. The specific volume, which is the sum of free volume and occupied volume [4], is therefore expected to decrease with increased extent of cure. However, the anomalous behavior of the material properties at room temperature suggests a more complicated situation [1-3]. In commercial practice this anomaly can result in a net expansion at room temperature when a reactive material which has been set at RT is post-cured at elevated temperatures and cooled to RT. Depending on the application, this can be either deleterious or advantageous.

Other studies on difunctional epoxy systems also have shown a lower density at room temperature to be associated with a higher glass transition temperature (T_g) [5-8] and a higher temperature of cure (T_c) [9]. Nevertheless, apparently conflicting results exist in the literature. For example, the room temperature density of a tetrafunctional epoxy system decreased on postcure [10], whereas in another report [11] the ρ_{RT} of the same, but epoxy-rich, system increased with increasing T_g.

In this work, the room temperature density of a difunctional epoxy monomer cured with a tetrafunctional aromatic diamine was studied as a func-

tion of both time and temperature of cure, and rate of cooling, in order to obtain more information on the anomalous behavior of cured thermosetting resins at room temperature. T_g is used as a measure of conversion. A preliminary report has been published [12].

EXPERIMENTAL

Materials & Specimen Preparation

The difunctional epoxy monomer employed was a diglycidyl ether of bisphenol A (DGEBA) (DER 331, Dow Chemical Co.) cured with a tetrafunctional aromatic diamine, trimethylene glycol di-p-aminobenzoate ("TMAB", Polarcure 740M, Polaroid Corp.) [3,12-16]. The chemical formulae of the reactants are shown in Figure 1. The materials were reacted stoichiometrically, one epoxy group with one amine hydrogen, according to their respective equivalent weights: DER 331, 190 gm/eq; TMAB, 78.5 gm/eq.

The difunctional epoxy monomer (a viscous liquid at 25°C) and curing agent (m.p. 125°C) were heated separately in beakers to 140°C. The epoxy monomer was added to the curing agent, and the mixture was stirred mechanically for 10 min at 140°C before being poured into aluminum dishes (each contained ~ 5 gm of the resin). These were stored in a dessicator in a freezer until needed (for making castings). About 10 gm of the resin mixture was dissolved in methyl ethyl ketone (1 gm solid/1 ml solvent) for use in torsional braid analysis (TBA) [17].

Cure Procedure

The procedure for obtaining disc-shaped cast specimens (average diameter ~ 5 mm; average thickness ~ 1 mm; average weight ~ 25 mg) from a mold follows. Before cure, a sample of the formulation in its aluminum dish was degassed at 110°C for 30 min (~ 1 torr). The degassed molten mixture was used to fill a multicavity aluminum mold (at 110°C) that was lined with an aluminum foil. The hot aluminum mold was then placed inside a copper block (~ 5 in. diameter) which had been preheated to the temperature of cure in a convection oven. All isothermal curing was conducted under a flowing atmosphere of nitrogen. Measurements of the time of cure started when the mold was placed in the oven. The aluminum foil was easily peeled off the cured specimens at RT.

Cooling Procedure

Two methods of cooling the oven-cured castings were used in this study. (a) For "slow-cool", specimens were allowed to cool freely inside the copper block to room temperature. The temperature change was monitored on a strip-chart recorder. Over the range of glass transition temperatures of interest, the cooling rate was different (but reproducible) from the various isothermal cure temperatures. It varied between 0.4°C/min at T_c = 180°C to 0.1°C/min at T_c = 100°C. However, for each isothermal temperature of cure, the rate of subsequent cooling varied less than 0.04°C/min over the range of glass transition temperatures being measured. This minimized the effect of different cooling rates at different T_gs which, with cooling rates increasing with increasing T_g, would have otherwise caused the density to decrease with increasing T_g, as has been suggested [18]. (b) For "fast-cool", specimens

were taken out of the cure oven, copper block and the aluminum mold, and were allowed to cool rapidly in air to room temperature (initial rate >> 1°C/min).

Density Measurements

The densities of the oven-cured specimens at 24.95°C (RT) were measured using a density gradient column [ASTM D1505 (19)] which had been prepared from toluene and carbon tetrachloride. The column was calibrated with density floats of 1.2045, 1.2106, 1.2196 and 1.2245 gm/ml. The sensitivity of the column was maintained at ± 0.0005 gm/ml-cm. Such sensitivity was needed to measure the change in RT density versus prehistory. The temperature of the density column was maintained at 24.95 ± 0.05°C using circulating water.

Prior to density measurements, specimens were examined between a pair of polarizers under a microscope. All the specimens used in this study were free from visible voids or bubbles that could affect the macroscopic density of the material.

Density measurements commenced within 5 minutes after isothermal cure and cooling to room temperature. Two to four specimens with the same prehistory were dropped into the density column and readings were taken after 20 minutes (at which time the location of each specimen had remained fairly constant for about 10 minutes). Reproducibility of density was ± 0.0001 g/ml. Since no two specimens had identical dimensions, no effect of specimen size on density was observed.

T_g Measurements

The glass transition temperatures of oven-cured and cooled disc-shaped cast specimens were measured in sealed sample pans using a differential

scanning calorimeter (Perkin-Elmer DSC-4) at 10°C/min under a helium atmosphere during the first heating scan. [Temperature calibration involved locating the melting point of a fresh Indium standard (156.6°C).] T_g was measured in the DSC curve as the point of intersection of the extrapolated baseline at the low temperature end and the tangent to the curve at the inflection point. Heats of reaction of unreacted and partially cured specimens were obtained from temperature scans from 10 to 350°C at 10°C/min (with subtraction of baselines) [16].

Torsional Braid Analysis (TBA)

Specimens, prepared by dipping heat-cleaned glass braids in the solution of reactants, were inserted in the apparatus which had been pre-set at the temperature of cure. Helium was used as the atmosphere. The times to gelation and vitrification were assigned from the maxima in logarithmic decrement vs. isothermal cure time plots, and used to construct an isothermal time-temperature-transformation (TTT) cure diagram, as shown in Figure 2. Two important temperatures were identified on the diagram: $_{gel}T_g$ and $T_{g\infty}$. The temperature $_{gel}T_g$ is defined as the isothermal cure temperature at which gelation and vitrification coincide (on a macroscopic scale); it was found to be approximately 67°C from the extrapolation of logarithmic times to gelation and vitrification vs. $1/T_C$ (K) plots [2,16]. Transition temperatures after isothermal cure were identified from the maxima in logarithmic decrement vs. temperature plots at scan rates of 1.5°C/min. $T_{g\infty}$, the maximum glass transition temperature obtained by isothermal cure, was ~170°C (~ 1 Hz) [15]. Materials cured above $T_{g\infty}$ will not vitrify during isothermal cure. Using the

TTT diagram as a framework, isothermal cure paths were designed to study the effect of cure on material properties at room temperature.

The epoxy system had been studied using the TBA dynamic mechanical technique for a preliminary report [15]. The automated TBA torsion pendulum system is available from Plastics Analysis Instruments, Inc.

RESULTS AND DISCUSSION

Dynamic Mechanical Measurements

A TBA dynamic mechanical spectrum of the material during isothermal cure at 100°C for 168 hours is shown in Figure 3. From the times to the maxima in the logarithmic decrement vs. log time plot, the times to gelation (t_{gel} ~ 401 min) and vitrification (t_{vit} ~ 729 min) are conveniently assigned. Cure proceeds beyond the assigned time to vitrification to eventually form a glass. A more appropriate time indicator for the formation of glassy-state material in principle is that at which the relative rigidity and mechanical damping "start" to level off. However, since the modulus and mechanical damping continuously change in the glassy state, an arbitrary and less reproducible index than the maximum in the logarithmic decrement would need to be selected.

The temperature scan for the material after cure at 100°C for 168 hours, and after cooling to -170°C, is shown in Figure 4. The scan from -170 to 240°C yields a T_g value of 130.2°C (~ 0.7 Hz). It can be observed that the location of the maximum in the logarithmic decrement is closer to the high temperature end of the transition region, and that the width of the glass

transition region (ΔT_g) is about 40°C (as demarcated by the arrows in Fig. 4). It is therefore not unusual that the T_g, as measured in this fashion after long cure times at T_c ($<< T_{g\infty}$), is higher than T_c by about 30°C. It follows that the material is in the glassy-state at T_c when $T_g > T_c + 30°C$. It has been shown that ΔT_g of the present system, which depends on the chemical and physical state of the material, is between 33 and 50°C [16]. However, for the purposes of discussion, the measured T_g is considered to be in the middle of the glass transition region and the cured material is considered to be a glassy solid when $T_g > T_c + 25°C$.

T_g vs. Time and Temperature of Isothermal Cure

Figure 5 is an example of a DSC thermogram of two specimens cured to different extents. The top curve is typical of all fast-cooled specimens which did not vitrify during cure, i.e., $T_g < T_c$. The bottom curve, which exhibits an endothermic enthalpy relaxation immediately above the assigned T_g, is typical of all slow-cooled, and also of fast-cooled specimens which had vitrified during cure. On heating through its glass transition temperature, an amorphous polymer regains the extra enthalpy that it has given up on aging in the glass transition region and in the glassy state and thus, an enthalpy relaxation is observed [20,21]. The methodology used to measure T_g results in the T_g appearing to increase with physical aging. Studies on various epoxy systems [10,22,23] have indicated that the enthalpy relaxation can be quantitatively related to the time of sub-T_g annealing.

Figure 6 is a plot of T_g vs. log time of cure obtained using DSC. For clarity, only the data at two temperatures of cure (100 and 180°C) are shown.

The top two curves are for T_c = 180°C and the bottom two curves for T_c = 100°C. It can be seen that the glass transition temperature of a slow-cooled specimen is greater than or equal to that of a fast-cooled specimen. This can be accounted for in terms of: (1) when the T_g of the material is lower than T_c, more cure can occur during cooling for the slow-cooled specimen than for the fast-cooled specimen, and therefore, T_gs are higher for the former; and (2) increased physical annealing on slow-cooling apparently yields higher glass transition temperatures [10,22-24]. When the material had vitrified during cure, as indicated by T_g being greater than T_c, its T_g is almost independent of the cooling rate since chemical and physical aging rates are very slow in the glassy state.

A summary of the T_g vs. time of cure data for fast-cooled specimens at different isothermal cure temperatures (100 to 180°C) is given in Figure 7. The T_g vs. time curves have been time-shifted using appropriate shift factors, A, such that the data fall on a master curve at the lower temperature end. This is based on the assumption that the cure reaction is under only kinetic control at low T_gs (i.e., low conversions where $T_g << T_c$) and that T_g is then a direct measure of conversion. Deviations from the composite curve occur when $T_g \geq T_c$ for cure temperatures of 100 and 120°C. This is indicative of diffusion-controlled processes. Similar results have been obtained based on conversion vs. time of cure at different isothermal cure temperatures [25,26]. The shift factors obey an Arrhenius relationship as is shown in Figure 8. An activation energy of approximately 15 kcal/mole is obtained from the slope of the straight line (the apparent activation energy obtained from the times to gelation using TBA was approximately 14 kcal/mole [16]).

Density at RT vs. Time and Temperature of Isothermal Cure

Figure 9a has plots of T_g (from DSC measurements) and density at RT vs. log time for isothermal cure at 80°C after cooling at the two rates. Similar results from T_c = 100 to 180°C are shown in Figures 9b-9f. The glass transition temperature is used as an index of the progress of cure. At T_c = 80°C, the RT density of both fast- and slow-cooled specimens was found to increase gradually with time of cure and appeared to level off when the material was in the glassy state at the temperature of cure (i.e., after $T_g > T_c + 25°C$). The initial increase in ρ_{RT} is the expected consequence of densification due to reaction in the liquid and rubbery states. Before the material had reached the glassy state during cure, the RT density of the fast-cooled specimens was lower than that of the slow-cooled specimens, for the same time of isothermal cure. This is again due to: (1) increased cure during slow-cooling resulting in further densification, and (2) increased physical annealing on slow-cooling yielding a higher density [10]. The latter is a manifestation of rate dependence in the glass transition region. However, after the material had formed a glass during isothermal cure, the values of RT density (and T_g) were approximately independent of the cooling rate. This is because the material was a glass at T_c and was cooled in the glassy state where the relaxation rates are low. It also follows that the coefficient of thermal expansion in the glassy state of the epoxy system is approximately independent of the cooling rate.

At T_c = 100°C (Fig. 9b), the RT density of fast-cooled specimens was also found to increase with cure. However, after an initial approximately constant level, the RT density of slow-cooled specimens <u>decreased</u> with

increasing cure: this is the principal anomaly. Two effects that can lead to lower RT densities with increasing conversion (i.e., T_g) are invoked. First, on cooling, the materials have diminished opportunities to contract in the liquid or rubbery state and so contraction occurs mostly in the glassy state with a lower coefficient of thermal contraction. This, in conjunction with the non-linear increase of T_g with conversion, can explain the anomaly (see later). Second, materials with a higher crosslink density, and thus with a higher T_g, may relax less completely than less crosslinked materials towards equilibrium on cooling through the glass transition region to RT. After isothermal vitrification, physical annealing occurs at the temperature of cure. Eventually both the fast- and slow-cooled specimens then had approximately the same density at RT, which again reflects that both materials effectively had the same thermal history.

The trend of decreasing density at RT with increasing time of cure (and T_g) is observed for both fast- and slow-cooled specimens at higher T_cs, as shown in Figures 9c - 9f.

As can be seen from Figures 9a - 9d, for cure temperatures at which isothermal vitrification can occur (i.e., $T_c < T_{g\infty}$), the RT density appears to reach a limiting value which decreases with increasing values of T_c. The limit is plausible as further shrinkage due to cure and physical densification in the glassy state is restricted at long times due to low mobility in the polymeric glass. Materials would be expected to have a higher specific volume on cooling to RT when cured at a higher temperature if the thermal expansion of the reacting resin is more dominant than the shrinkage due to cure [9]. However, when the material is "fully" reacted by curing above its

T_{g^∞}, its density at RT is independent of T_c for a given cooling rate (see Fig. 11). This argues against the pertinence of thermal motion in controlling the density of the present system at the temperature of cure. In the absence of vitrification, it is the conversion that controls the density.

At T_c = 180°C (Fig. 9f), the reaction rate was so fast that high conversions were reached prior to measuring T_g, which therefore did not appear to change significantly. Similarly, no significant change in RT densities was observed. When the material is cured above its T_{g^∞}, it does not vitrify during cure and subsequent cooling from T_c occurs through the rubbery and glassy states. Again, the transition from the rubbery to the glassy state is highly rate dependent which leads to the physical parameters in the glassy state being dependent on the rate of cooling, as shown in Figures 9e and 9f.

Density at RT vs. T_g

Figure 10 is a summary of the RT density of slow-cooled specimens vs. (T_g - RT) at different isothermal cure temperatures (66.7 to 200°C). The temperature $_{gel}T_g$ is used as a demarcation: materials to the left of the dashed line have not gelled during cure, whereas those to the right have. (As a caveat, $_{gel}T_g$, which is a macroscopic parameter, is intended only as a qualitative indicator for the microscopic gelation process.) It can be seen that ρ_{RT} increases with T_g prior to gelation, reaches a maximum value after gelation, and begins to decrease with further cure. It has been reported earlier that the density (at 25°C) of a DGEBA epoxy resin cured with phthalic acid anhydride increased with time of cure at a single cure temperature, reached a maximum value in the vicinity of the gel point, and then decreased

on further cure [9]. The general shape of a "master" curve is evident in Figure 10 which in effect shows the maximum in the one-to-one relationship between ρ_{RT} and conversion in the absence of vitrification on cure. It is difficult experimentally to obtain the complete curve based on one cure temperature as the reaction rate is too fast at high T_cs and isothermal vitrification limits the extent of cure at low T_cs. Perturbations occur when $T_g \geq T_c$ (as indicated by the arrows in Figure 10). The vitrification process is accompanied by an increase in density due to physical aging which competes with the decrease in RT density due to chemical aging (cure). Vitrification nullifies the unique relationship between ρ_{RT} and conversion. The same value of T_g, as measured by DSC, can then arise from different combinations of conversion and extent of physical annealing.

As indicated by the enthalpy relaxation measured during DSC studies (Fig. 3), physical annealing occurs in the glass transition region and in the glassy state. However, even at T_c it cannot reverse the trend of decreasing ρ_{RT} with increasing conversion.

The limiting RT density, that corresponds to the highest T_g attained after long times (~ 2 weeks) at each T_c vs. T_c, for slow-cooled specimens is shown in Figure 11. From T_c = 66.7 to 140°C, the relationship appears to be linear. The materials are at different chemical and physical states when vitrified at different T_cs. When the material is fully cured at $T_c \geq T_{g\infty}$ (i.e., without vitrifying), its RT density (Fig. 11) and T_g (Fig. 10) for a given cooling rate appear to be independent of T_c, thus reflecting the same chemical and physical state. Control and variation of density at room temperature by appropriate cure conditions is of importance in commercial appli-

cations requiring dimensional stability. When T_g is high the limiting room temperature density will be stable if the cooling rate is very slow.

A similar trend of decreasing RT density with increasing T_g beyond gelation is observed for the fast-cooled specimens (Fig. 12) for different isothermal cure temperatures (80 to 180°C). Comparison of Figures 10 and 12 shows that the RT density, and its behavior with respect to conversion, are dependent upon the cooling rate through the glass transition when the material has not vitrified during cure. Scrutiny of the literature reveals that the rate of cooling is not always reported (or measured). This information is particularly important where quenching is employed to study, on a time basis, the effect of cure on material properties, such that, further cure on cooling has been minimized.

Volume-Temperature Relationship of Amorphous Polymers

The specific volume (V)-temperature (T) relationship for an amorphous polymer is shown schematically in Figure 13. The following parameters can be defined from the slopes of the V vs. T curves:

$$E_\ell = [V(T_c) - V(T_g)]/(T_c - T_g) \quad (1)$$

$$E_g = [V(T_g) - V(RT)]/(T_g - RT) \quad (2)$$

where $V(T_c)$ = specific volume at temperature of cure

T_c = temperature of cure

$V(T_g)$ = specific volume at T_g

$V(RT)$ = specific volume at RT

The V vs. T curves at different degrees of cure will be parallel to one another

(below and above the glass transition temperature, respectively) for materials in which the expansion coefficients in the rubbery and glassy states do not change with cure [7,9,16].

Combining eqs. (1) and (2) and rearranging, gives the specific volume at RT:

$$V(RT) = V(T_c) - E_\ell(T_c - T_g) - E_g(T_g - RT) \qquad (3)$$

The anomalous V(RT) vs. T_g behavior observed is represented schematically in Figure 14. The anomaly corresponds to a positive slope of $V(T_g)$ vs. T_g relative to E_g (Fig. 14, dashed line) [3,7]. Assuming the constancy of E_ℓ and E_g versus conversion, which appears to be valid for the present [16] and other epoxy systems [7,9], eq. (3) can be differentiated with respect to the extent of cure, p,

$$dV(RT)/dp = dV(T_c)/dp + (E_\ell - E_g)dT_g/dp \qquad (4)$$

As shrinkage is usually associated with the cure of epoxies, $dV(T_c)/dp$ is negative. dT_g/dp and $(E_\ell - E_g)$ are always positive. Therefore, according to eq. (4), the specific volume at RT can either decrease, remain unchanged or increase with cure depending on the relative magnitudes of $dV(T_c)/dp$ and $(E_\ell - E_g)dT_g/dp$.

Cure of difunctional epoxy resins with methylene dianiline and 4,4'-diamino diphenyl sulfone (DDS) has shown (using volume dilatometry) that the total shrinkage due to full cure was less than 10 percent when measured at the temperatures of cure [6]. It has been suggested that most of this shrinkage arises from the better packing of network chains due to their higher connec-

tivity [27]. However, it has also been suggested that the rigidity of the network chains prevents the free volume from collapsing as much as would be expected during cure at high conversions [7]. (It is difficult to quantify free volume [28,29].) Although the magnitude of $dV(T_c)/dp$ is small, it is comparable to that of $(E_\ell - E_g)dT_g/dp$ (see below).

The glass transition temperature is an important parameter as a material can contract on cooling in the rubbery state only when its T_g is less than the temperature of cure. As the T_g increases with cure, the contraction in the rubbery state is diminished. Accordingly, materials with a higher T_g assume more contraction in the glassy state but with a lower thermal coefficient than that in the rubbery state.

Figure 15 shows data for T_g vs. conversion for the fast-cooled specimens. The degree of cure was obtained from the residual exotherm of a partially cured specimen in comparison with the total heat of reaction of an unreacted sample, as measured by DSC at 10°C/min. It is apparent the glass transition temperature increases more rapidly with increasing conversion for epoxies after the gelation point [11, 13, 30-32]. This can be explained for the present system in terms of the concentration of trifunctional and tetrafunctional crosslinking units which is calculated, using a recursive theory [33], as a function of extent of cure and shown in Figure 16 [33]. After the chemical gelation point [34] [see eq. (5) with f = 4],

$$P_{gel} = \frac{1}{[1 + (f-2)]^{\frac{1}{2}}} = 0.577 \qquad (5)$$

it appears that the glass transition temperature, which reflects the long range mobility of network chains, is influenced especially by the concentration of the

highest crosslinked units in the network. This consequence has been predicted in terms of free volume arguments for polymer networks [35].

These results emphasize the merit of using the glass transition temperature as a measure of the extent of reaction [15]. T_g, as a parameter by itself, is easily and accurately measured, and renders itself particularly informative in the later stages of cure (e.g., conversion > 90%), whereas conventional techniques such as FTIR and DSC are less sensitive at high conversion for measuring the change in degree of cure with time (see later). However, it is again noted that T_g, depending on how it is measured, can be affected by physical as well as chemical aging.

In the following calculation, the comparable magnitude of the terms, $dV(T_c)/dp$ and $(E_\ell - E_g)dT_g/dp$, in eq. (4) is demonstrated with relevant data in the literature. Average numerical values of dT_g/dp are calculated before and after gelation.

For the present system, before gelation,

$$dT_g/dp = ({}_{gel}T_g - T_{go})/(p_{gel} - 0) = (67 - 13)/(0.577 - 0) = 93.6 \text{ K} \quad (6)$$

where $T_{go} = T_g$ of the unreacted resin = 13°C (as measured by DSC at 10°C/min [16]). Thus,

$$(E_\ell - E_g)dT_g/dp = (3.3 \times 10^{-4})(93.6) \simeq 0.03 \text{ cm}^3/\text{gm} \quad (7)$$

After gelation,

$$dT_g/dp = (T_{g\infty} - {}_{gel}T_g)/(1 - p_{gel}) = (170 - 67)/(1 - 0.577) = 243.5 \text{ K} \quad (8)$$

Thus,

$$(E_\ell - E_g)dT_g/dp = (3.3 \times 10^{-4})(243.5) \simeq 0.08 \text{ cm}^3/\text{gm} \quad (9)$$

The total volume shrinkage due to complete cure for a DGEBA cured with DDS, which has a similar molecular weight between crosslinks as the present system, is about 8% [6,36]. Thus,

$$\left|\frac{dV(T_c)}{dp}\right| = 0.08\ V(T_c) \sim 0.07 \text{ cm}^3/\text{gm}. \quad (10)$$

For DGEBA systems with lower crosslink densities, the total shrinkage is smaller as the number of covalent bonds formed per unit volume is smaller [36], which results in a lower numerical value of $dV(T_c)/dp$.

Therefore, in the later stages of cure, it appears that the effect of increase in T_g due to increased extent of cure can become more dominant than the effect of cure shrinkage. Consequently, according to eq. (4), the specific volume at RT can increase with increasing T_g as the shrinkage at T_c is smaller than the loss of contraction on cooling in the rubbery state due to a higher T_g.

A merit of using eq. (4) in elucidating the anomaly lies in its ability to predict a maximum in RT density with increasing conversion in the vicinity of gelation. In previous studies, the following free volume arguments have been employed in different contexts to explain the inverse relationship between RT density and T_g: (1) the higher its T_g, the further from equilibrium the material is at RT, and thus, more free volume at RT [2,37]; (2) the decrease in free volume (and occupied volume) at T_c is less than expected due to steric hinderence [3,7], and (3) a higher crosslink density leads to a lower molecular mobility (which is not compensated by the higher value of the glass transition temperature) and thus to a reduced kinetic ability to closely pack during

cooling to RT [38]. The mechanism of attaining the "extra" free volume is different in each of the above arguments. Nevertheless, the outcome is the same, namely, a larger RT free volume being associated with a higher glass transition temperature and a positive slope of $V(T_g)$ vs. T_g relative to that of the glassy state (dashed line in Fig. 14).

As a caveat, it is noted that a macroscopic density technique does not measure the free volume directly. However, a free volume consideration can be shown to be consistent in the following manner. Accordingly, the increase in free volume at RT, $\Delta V_f(RT)$, due to increased conversion, can be equated to the increase in total volume at RT (i.e., approximately 0.5%, as in Fig. 10)

$$\Delta V_f(RT) = 0.005V(RT) \tag{11}$$

The free volume at T_g is considered to be about 2.5% of the total volume [4]. Therefore $V_f(RT) \simeq 0.025V(RT)$. Thus from eq. (11), the fractional free volume increase at RT caused by increasing conversion is approximately

$$\Delta V_f(RT)/V_f(RT) \simeq [0.005V(RT)]/[0.025V(RT)] \simeq 0.2 \tag{12}$$

After postcure, the RT moduli of many epoxy systems [2,3,13,16,39] have been found to decrease by the same magnitude. This suggests that the modulus is inversely related to the free volume [38]. A similar increase in the equilibrium level of water absorbed at RT was also found for epoxy systems [3].

Non-Equilibrium Nature of the Glassy State

The volume-temperature relationship depicted in eq. (3) does not explicitly take into account the non-equilibrium nature of materials below their

glass transitions. Amorphous materials in the glassy state can be considered to be supercooled liquids or supercooled rubbers whose volume and enthalpy are in excess when compared to the "equilibrium glass". The approach towards equilibrium by cooling through the glass transition region, in principle, can only be attained by an infinitely slow rate.

As shown in Figure 10, the density at RT decreases with increasing T_g after the gelation point. The parameter, (T_g - RT), can be considered as an index of departure from equilibrium at RT. In general, the higher the glass transition temperature, the further away is from the equilibrium state at RT. [2,37].

The slow approach to equilibrium, which can be measured in DSC studies in terms of enthalpy relaxation (Fig. 3), is observed in all slow-cooled, as well as fast-cooled specimens which have vitrified during cure. This implies that physical densification can occur either isothermally, as the glass transition region rises slowly through the temperature of reaction, or by slow-cooling through the glass transition region. Earlier studies on the stress relaxation of crosslinked rubber [40] showed that the relaxation times were strongly dependent on the crosslink density. The immediate effect is that, given the same rate of cooling, the degree of relaxation through the glass transition region will be different for materials crosslinked to different extents. It follows that although a material with shorter relaxation times on cooling through the glass transition region will be denser at RT than that of a material with longer relaxation times, at RT the former will densify (i.e., physically age) more slowly than the latter. Therefore, it is important to understand the relationship between chemical structure (e.g., crosslink density) and relaxation

times for epoxies with different degrees of cure [6,36]. Consequently, the key issue that needs to be addressed is whether the "anomaly" that is observed is due entirely to the non-equilibrium behavior of the material below its glass transition temperature. In other words, can the trend of decreasing density with increasing conversion (T_g) be reversed by physical annealing? Or does the change in chemical structure per se (e.g., crosslink density) result in more free volume in the glassy state. If the non-linear increase in T_g with conversion after the gel point (Fig. 15) is itself the consequence of longer relaxation times being associated with a higher crosslink density, then the two ways of explaining the anomaly will have been unified.

In the literature [10,20,22,23,29], sub-T_g annealing studies usually involve the initial quenching of materials from an equilibrium state ($T \geq T_g + 25°C$) to a non-equilibrium state (e.g., $T < T_g - 25°C$). The material properties in the glassy state are then measured as a function of isothermal annealing time. The quenching process inevitably causes extra free volume to be entrapped in the polymer network. The subsequent densification process involves the gradual decrease of free volume towards the equilibrium value. Therefore, the thermal prehistory of an amorphous glass is a pertinent factor in determining the initial mobility of the molecular segments, and subsequently, the rate of the annealing process.

To study the physical aging of a fully cured material is straight forward; however, the same cannot be said for a partially cured material. The latter is complicated in the present system by chemical aging that can occur during the slow cooling (or heating) through the glass transition. Therefore, the following preliminary discussion deals with fully reacted materials.

Physical Aging Studies

A "fully" cured material (T_g = 165°C), cured at 180°C for 24 hr, was quenched in nitrogen from 220°C at approximately 55.6°C/min (100°F/min) to 139°C and was annealed in nitrogen at 139°C for different times. After specific times of annealing, the aged material was "fast-cooled" in air to room temperature and its density at RT was measured. The change in RT density with time of annealing is depicted in Figure 17. It can be seen that the densification process at 139°C is quite rapid in the early stages. The density seems to reach an asymptotic value after 24 hours. The density at long times is about that of the same material when cooled slowly to RT (~ 0.4°C/min) from above $T_{g\infty}$ (Fig. 9f). This suggests that the RT density obtained by the slow-cool process is close to the upper boundary of the material. When the annealed material was rejuvenated by heating to 220°C and quenched in nitrogen to RT (> 50°C/min), the density at RT was approximately the same as the preaged and quenched material (± 0.0001 gm/ml). This demonstrates the thermo-reversibility of the physical process.

Also shown in Figure 17 is the RT density vs. time profile of a fully cured material with a different cure history (cured at 169°C for 64 hr) that was quenched from 220°C at 100°F/min to 36°C and annealed at 36°C, before being cooled slowly to RT. Apparently, the molecular mobility of the polymer network is low at the annealing temperature and only an uncertain change in the macroscopic density at RT is observed. However, more obvious changes have been observed by dynamic mechanical measurements [16] which are more sensitive to molecular processes than the present density column method.

Currently, the effects of different thermal prehistories and annealing temperatures on the dynamic mechanical properties are being investigated [16].

CONCLUSIONS

The RT density and T_g of a diglycidyl ether of bisphenol A cured with a tetrafunctional aromatic diamine has been investigated as a function of time and temperature of isothermal cure, and cooling rate.

The room temperature density passes through a maximum value with increasing conversion when cure is performed at elevated temperatures. For prescribed cooling rates, cure results in a unique value of ρ_{RT} for a given conversion as long as the material does not vitrify on cure. The occurrence of vitrification during cure eliminates the one-to-one relationship because of physical aging in the glass transition region. Prolonged isothermal cure to well beyond vitrification results in limiting values of ρ_{RT} which decrease with increasing temperature of cure. The maximum in the ρ_{RT} vs. conversion relationship is discussed in terms of: (1) competition between shrinkage due to isothermal cure, and loss of contraction on cooling in the rubbery state due to the non-linearly increasing values of T_g, and (2) physical annealing in the glass transition region being more efficient for materials with lower values of T_g.

The effect of annealing on the RT density of fully cured materials has also been considered. However, it is not conclusive as to whether physical annealing can eventually reverse the trend of decreasing RT density with increasing conversion. Complications include the relaxation times being much longer than the time scale being studied, and the spectrum of relaxation times being dependent on the molecular structure (e.g., crosslink density).

It is pertinent to study the effect of crosslink density, annealing temperatures and thermal prehistories on the annealing process before volume-

temperature relationships in the glassy state of thermosetting systems can be fully understood.

Acknowledgements. Financial support has been provided by the Office of Naval Research, the State of New Jersey Governor's Commission on Science and Technology (Contract Number 85-990690-9), and the Princeton Plasma Physics Laboratory.

REFERENCES

[1] J. P. Aherne, J. B. Enns, M. J. Doyle and J. K. Gillham, Amer. Chem. Soc., Div. Org. Coat. Plast. Chem., Prepr., 46, 574 (1982).

[2] J. B. Enns and J. K. Gillham, J. Appl. Polym. Sci., 28, 2831 (1983).

[3] M. T. Aronhime, X. Peng and J. K. Gillham, J. Appl. Polym. Sci., 32, 3589 (1986).

[4] J. D. Ferry, "Viscoelastic Properties of Polymers", 3rd ed., Wiley, New York, 1980.

[5] V. B. Gupta, L. T. Drzal and M. J. Rich, J. Appl. Polym. Sci., 30, 4467 (1985)

[6] I. C. Choy and D. J. Plazek, J. Polym. Sci.: Part B: Polym. Phys., 24, 1303 (1986).

[7] A. Shimazaki, J. Polym. Sci., Part C, 23, 555 (1968).

[8] K. Suzuki, Y. Miyano and T. Kunio, J. Appl. Polym. Sci., 21, 3367 (1977).

[9] W. Fisch, W. Hofman and R. Schmid, J. Appl. Polym. Sci., 13, 295 (1969).

[10] E. S. W. Kong, "Epoxy Resins and Composites IV", K. Dusek, ed., Advances in Polymer Science, Vol. 80, pp. 125-172, Springer-Verlag, New York, 1986.

[11] M. Cizmecioglu, A. Gupta and F. R. Fedors, J. Appl. Polym. Sci., 32, 6177 (1986).

[12] K. P. Pang and J. K. Gillham, Amer. Chem. Soc., Proceedings Div. Polym. Mat.: Sci. Eng., 56, p. 435, 1987.

[13] L. C. Chan, H. N. Naé and J. K. Gillham, J. Appl. Polym. Sci., 29, 3307 (1984).

[14] X. Peng and J. K. Gillham, J. Appl. Polym. Sci., 30, 4685 (1985).

[15] K. P. Pang and J. K. Gillham, Amer. Chem. Soc., Proceedings Div. Polym. Mat: Sci. Eng., 55, 64, 1986.

[16] K. P. Pang, Ph.D. dissertation, Department of Chemical Engineering, Princeton University, 1988.

[17] J. B. Enns and J. K. Gillham, Amer. Chem. Soc., Adv. Chem. Ser., 203, 27 (1983).

[18] J. K. Gillham, Polym. Eng. Sci., 26, 1429 (1986).

[19] 1965 ASTM Standards, Part 27, p. 500, ASTM Philadelphia, 1965.

[20] S. E. B. Petrie, Bull. Am. Phys. Soc., 17, 373 (1972).

[21] S. E. B. Petrie, "Physical Structure of the Amorphous State", G. Allen and S. E. B. Petrie, eds., pp. 225-247, Marcel Dekker, New York, 1977.

[22] Z. H. Ophir, J. A. Emerson and G. L. Wilkes, J. Appl. Phys., 49, 5032 (1978).

[23] M. Mijovic and K. F. Lin, J. Appl. Polym. Sci., 32, 3211 (1986).

[24] R. A. Fava, Polymer, 9, 137 (1968).

[25] M. J. Acitelli, R. B. Prime and E. Sacher, Polymer, 12, 333 (1971).

[26] S. Lunak, J. Vladyka and K. Dusek, Polymer, 19, 931 (1978).

[27] E. F. Oleinik, "Epoxy Resins and Composites IV", K. Dusek, ed., Advances in Polymer Science, Vol. 80, pp. 49-99, Springer-Verlag, New York, 1986.

[28] Y. Lipatov, "Confirmation and Morphology", Advances in Polymer Sci., Vol. 76, pp. 63-104, Springer-Verlag, New York, 1978.

[29] L. C. E. Struik, "Physical Aging in Amorphous Polymers and Other Materials", Elsevier, Amsterdam, 1978.

[30] H. E. Adabbo and R. J. J. Williams, J. Appl. Polym. Sci., 27, 1327 (1982).

[31] J. B. Enns and J. K. Gillham, J. Appl. Polym. Sci., 28, 2567 (1983).

[32] S. A. Bidstrup, N. F. Sheppard, Jr. and S. D. Senturia, Office of Naval Research Contract N00014-84-K-0274, Technical Report No. 8, November 15, 1986.

[33] D. R. Miller and C. W. Macosko, Macromolecules, 9, 206 (1976).

[34] P. J. Flory, "Principles of Polymer Chemistry", Cornell University Press, Ithaca, N.Y., 1953.

[35] A. J. Chompff, "Polymer Networks, Structure and Mechanical Properties", A. J. Chompff and S. Newman, eds., pp. 145-192, Plenum Press, New York, 1971.

[36] I. C. Choy, Ph.D. dissertation, Materials Science and Engineering Department, University of Pittsburgh, 1987.

[37] J. K. Gillham, Polym. Eng. Sci., 19, 676 (1979).

[38] A. Noordam, J. J. M. H. Wintraecken and G. Walton, "Crosslinked Epoxies", B. Sedlacek and J. Kahovec, eds., pp. 373-389, Walter de Gruyter & Co., New York, 1987.

[39] L. C. Chan, J. K. Gillham, A. J. Kinloch and S. J. Shaw, "Rubber-Modified Thermoset Resins", C. K. Riew and J. K. Gillham, eds., Amer. Chem. Soc., Adv. Chem. Ser., 208, 235 (1984).

[40] D. J. Plazek, J. Polym. Sci., A-2, 4, 745 (1966).

FIGURE CAPTIONS

Fig. 1 Chemical formulae of the difunctional epoxy (DER331)/tetrafunctional aromatic amine (TMAB) system.

Fig. 2 Time-temperature-transformation (TTT) cure diagram for DER 331/TMAB: (⊡) gelation (experimental); (◆) vitrification (experimental). $T_{g\infty}$ is the maximum value of T_g (~ 170°C) obtained by isothermal cure. $_{gel}T_g$ is the cure temperature (~ 67°C) at which gelation and vitrification occur simultaneously. Data were obtained using TBA.

Fig. 3 Dynamic mechanical spectrum (TBA) of DER 331/TMAB during isothermal cure at 100°C for 168 hours: (□) relative rigidity, and (◆) logarithmic decrement.

Fig. 4 Dynamic mechanical spectrum (TBA) of DER 331/TMAB versus temperature after cure at 100°C for 168 hours: (□) relative rigidity, and (◆) logarithmic decrement. Arrows indicate the limits of the glass transition. Scanning rate: +1.5°C/min in dry helium.

Fig. 5 Differential scanning calorimetry (DSC) traces of fast-cooled (dashed line) and slow-cooled (solid line) specimens during the first heating scan. Heating rate: 10°C/min. The procedure for assigning values to the glass transition temperature is indicated.

Fig. 6 T_g vs. log time of cure: (⊡) slow-cooled from 180°C; (◆) fast-cooled from 180°C; (■) slow-cooled from 100°C and (◇) fast-cooled from 100°C. T_g was determined using DSC.

Fig. 7 T_g vs. log (shifted) time of cure for fast-cooled specimens at different isothermal cure temperatures: (□) 100°C; (◆) 120°C; (△)

140°C; (◇) 165°C, and (■) 180°C. T_g was determined using DSC.

Fig. 8 Arrhenius analysis of the shift factors used in Figure 7.

Fig. 9 T_g and density at RT vs. log time for isothermal cure at various temperatures: (a) 80°C; (b) 100°C; (c) 120°C; (d) 140°C; (e) 165°C and (f) 180°C. (⊡) slow-cooled specimens, and (◆) fast-cooled specimens. T_g was determined using DSC.

Fig. 10 RT density of slow-cooled specimens vs. (T_g - RT) for different isothermal cure temperatures: (△) 66.7°C; (▲) 80°C; (□) 100°C; (◈) 120°C; (■) 140°C; (◘) 165°C; (◆) 180°C, and (⊡) 200°C. Arrows indicate the vitrification points where $T_g = T_c$. $_{gel}T_g$ (dashed line) is used as a demarcation between ungelled and gelled specimens.

Fig. 11. Limiting RT density for slow-cooled specimens vs. T_c.

Fig. 12. RT density of fast-cooled specimens vs. (T_g - RT) for different isothermal cure temperatures: (▲) 80°C; (□) 100°C; (◈) 120°C; (■) 140°C; (◘) 165°C, and (◆) 180°C. Arrows indicate the vitrification points where $T_g = T_c$. $_{gel}T_g$ (dashed line) is used as a demarcation between ungelled and gelled specimens.

Fig. 13. Schematic specific volume(V)-temperature(T) diagram for amorphous glassy polymers.

Fig. 14. Schematic specific volume(V)-temperature(T) diagram of epoxies cured to different extents (1 < 2 < 3) at T_c. Note the anomalous behavior of increasing volume at RT with increasing T_g when T_g >> RT. $V(T_g)$ vs. T_g for T_g >> RT is represented by the dashed line [3,7].

Fig. 15. T_g vs. conversion at various T_cs using DSC: (▲) 66.7°C;

(◆) 80°C; (□) 100°C; (◇) 120°C; (■) 140°C; (X) 165°C, and (+) 180°C.

Fig. 16. Population density of crosslinked units vs. extent of cure; (□) $P(X_{3,4})$, is the probability that three of the four branches of the crosslinking units are connected; (◆) $P(X_{4,4})$, is the probability that all four of the branches are connected, and (■) [X], is the total crosslink density, i.e., the sum of $P(X_{3,4})$ and $P(X_{4,4})$.

Fig. 17. Density at RT vs. time of annealing at two annealing temperatures: (□) 139°C, and (◆) 36°C.

Chemical Formulae

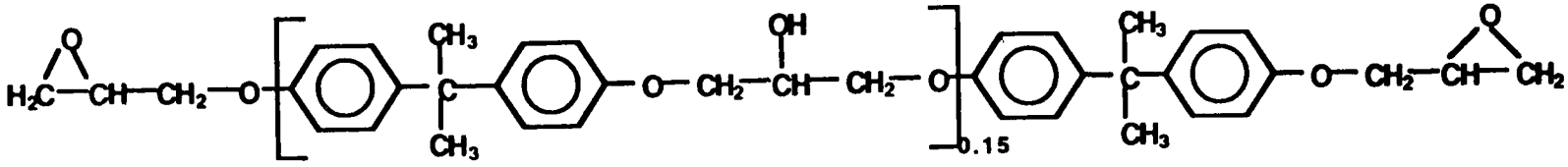

Diglycidyl Ether of Bisphenol A [DER 331]

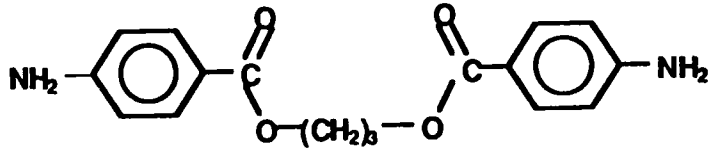

Trimethylene Glycol Di-p-aminobenzoate [TMAB]

Figure

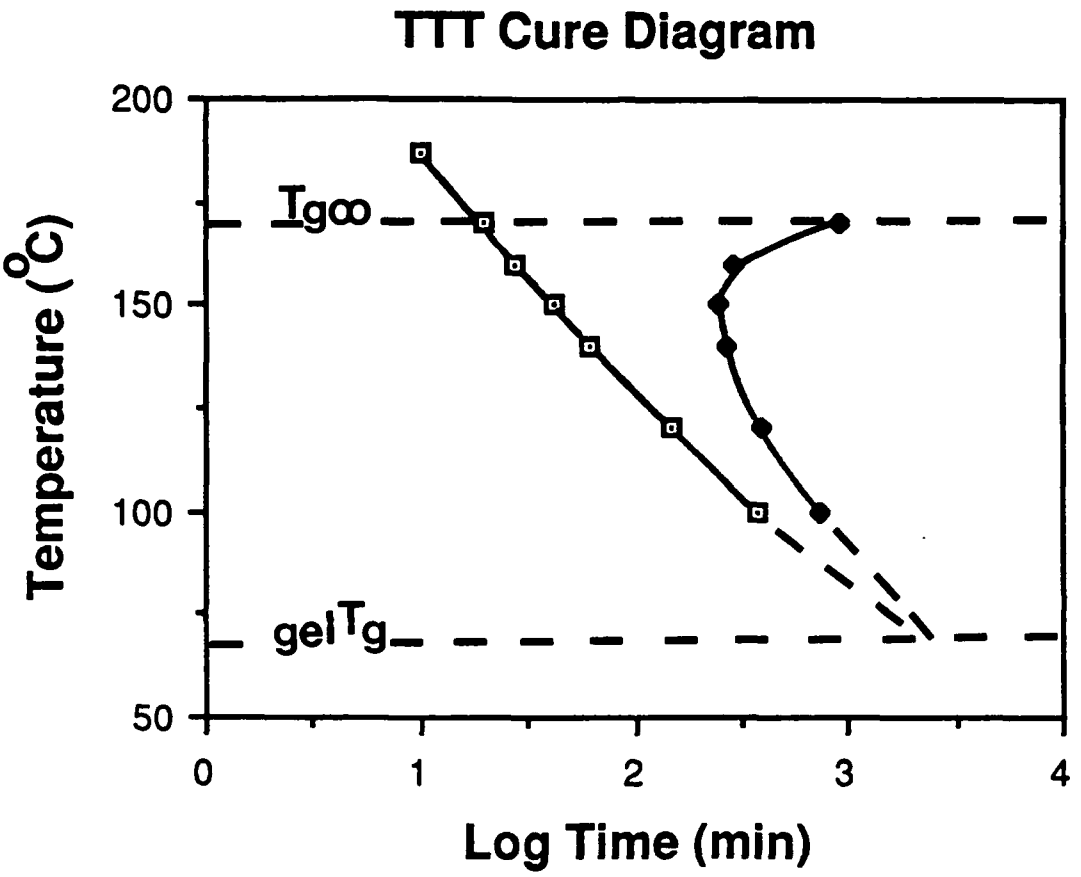
TTT Cure Diagram
200
150
100
50
Temperature (°C)
$T_{g\infty}$
gel T_g
0
1
2
3
4
Log Time (min)

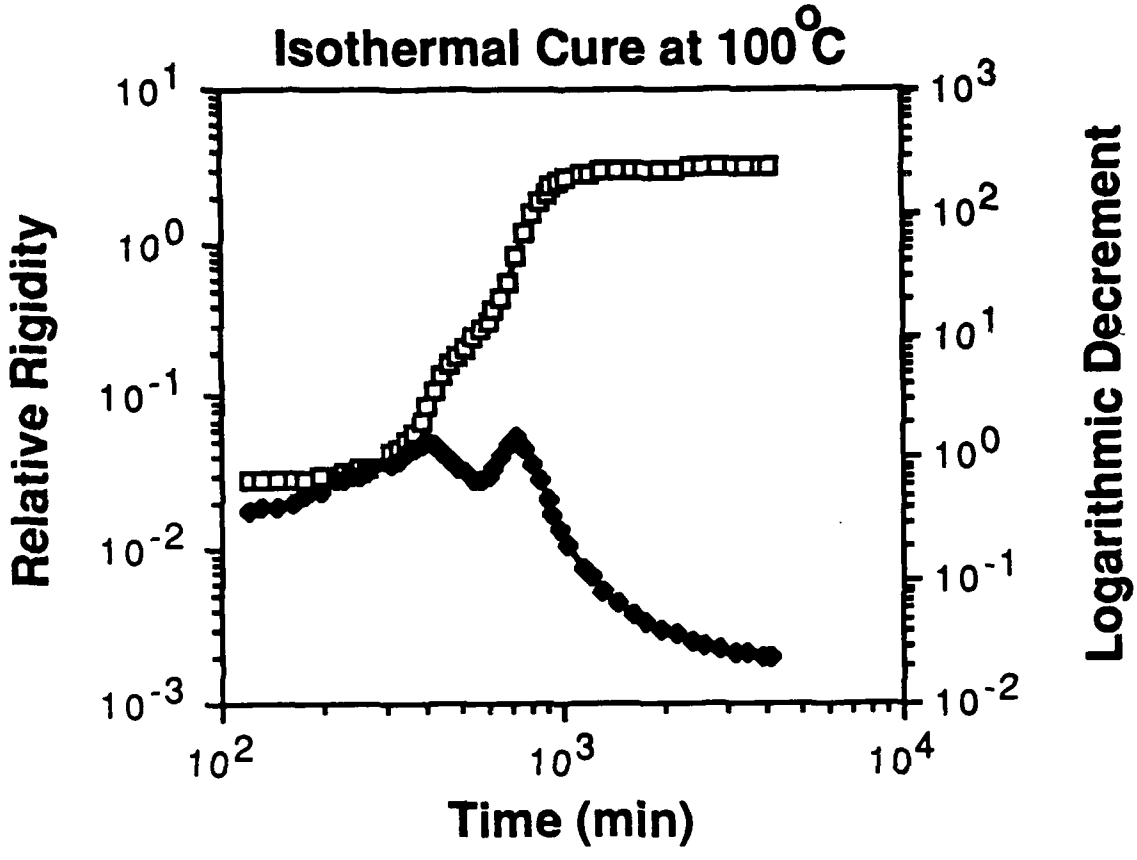
Isothermal Cure at 100°C
Relative Rigidity
Logarithmic Decrement
Time (min)
10^1
10^0
10^-1
10^-2
10^-3
10^3
10^2
10^1
10^0
10^-1
10^-2
10^2
10^3
10^4

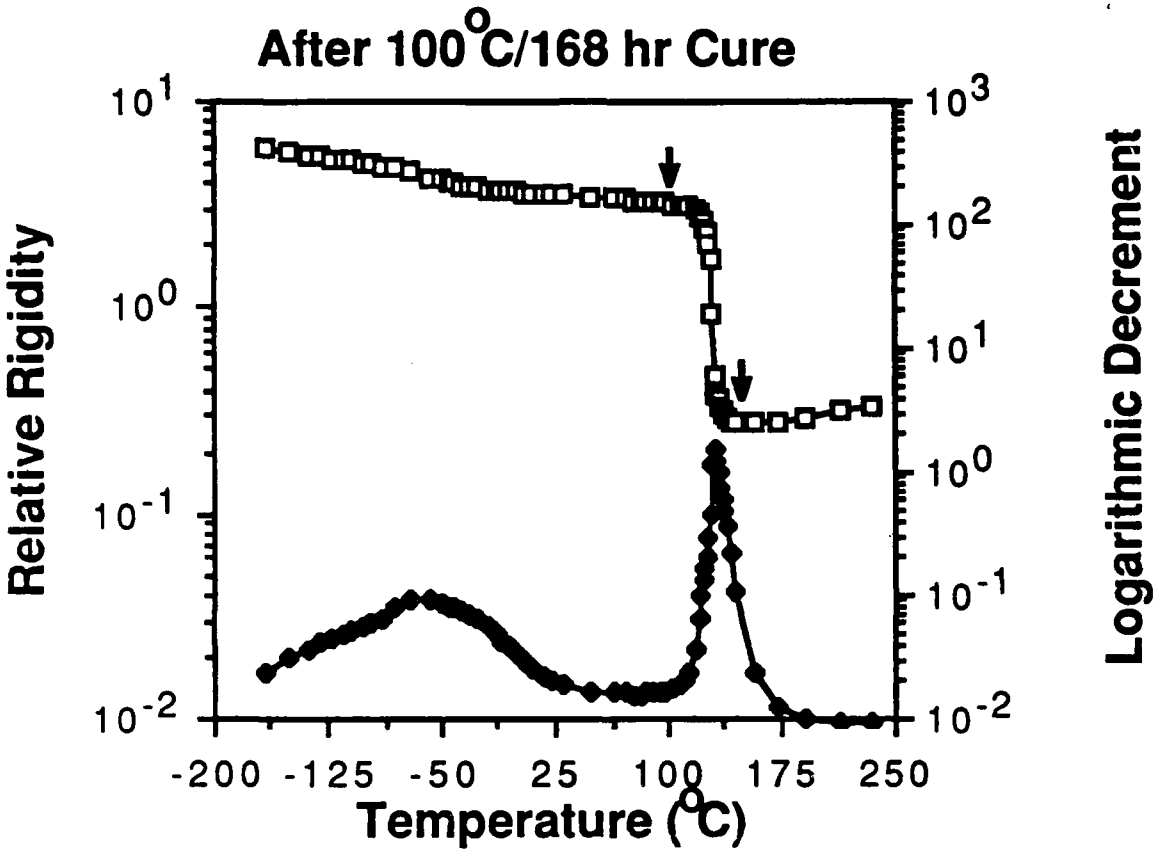
After 100°C/168 hr Cure
Relative Rigidity
Logarithmic Decrement
10^1
10^0
10^-1
10^-2
10^3
10^2
10^1
10^0
10^-1
10^-2
-200 -125 -50 25 100 175 250
Temperature (°C)

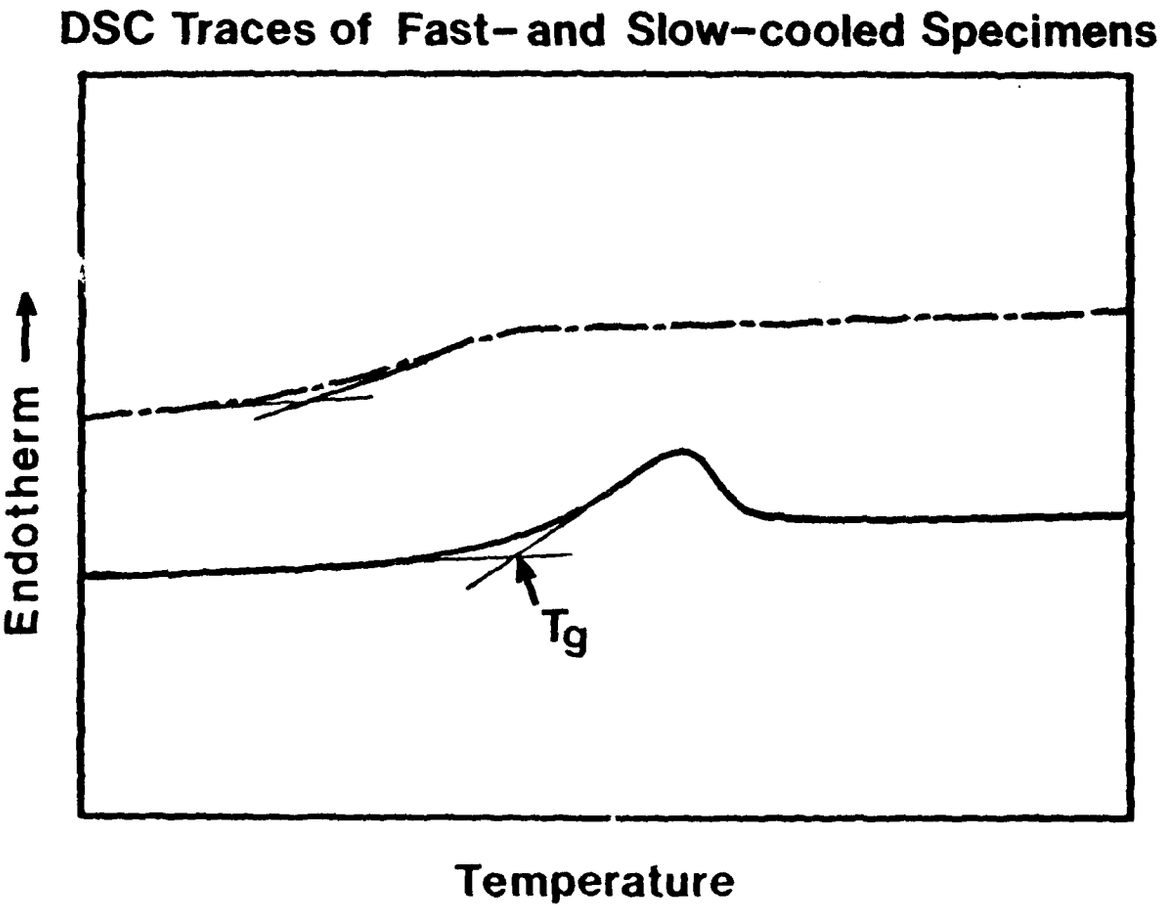
DSC Traces of Fast-and Slow-cooled Specimens
Endotherm
Tg
Temperature

Figure

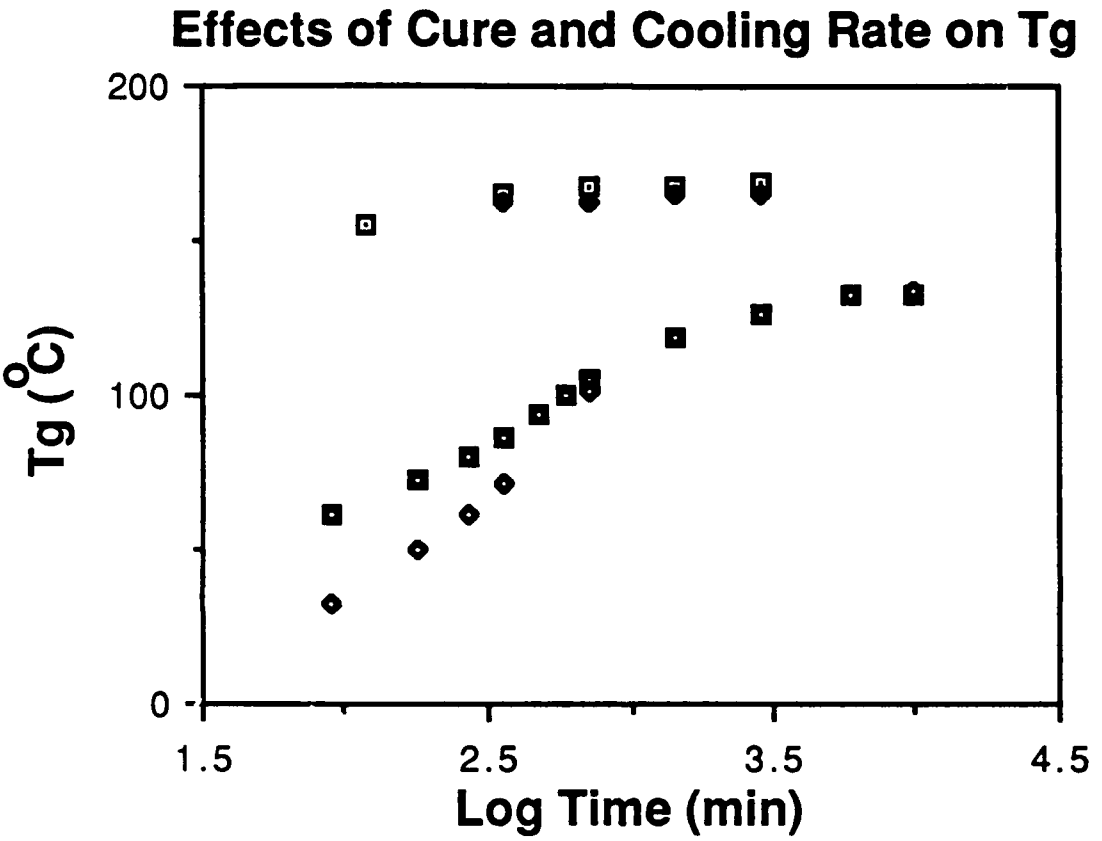
Effects of Cure and Cooling Rate on Tg
200
100
0
Tg (°C)
1.5
2.5
3.5
4.5
Log Time (min)

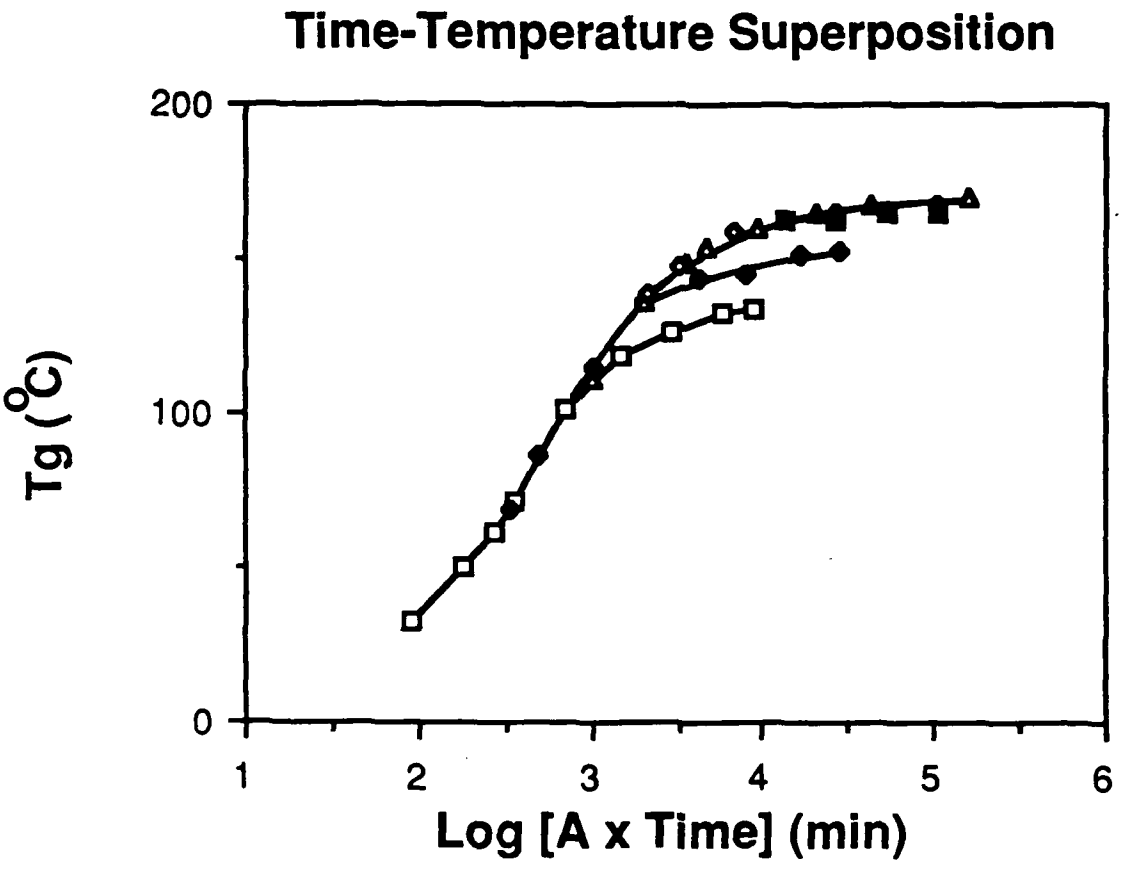
Time-Temperature Superposition
200
100
0
Tg (°C)
1
2
3
4
5
6
Log [A x Time] (min)

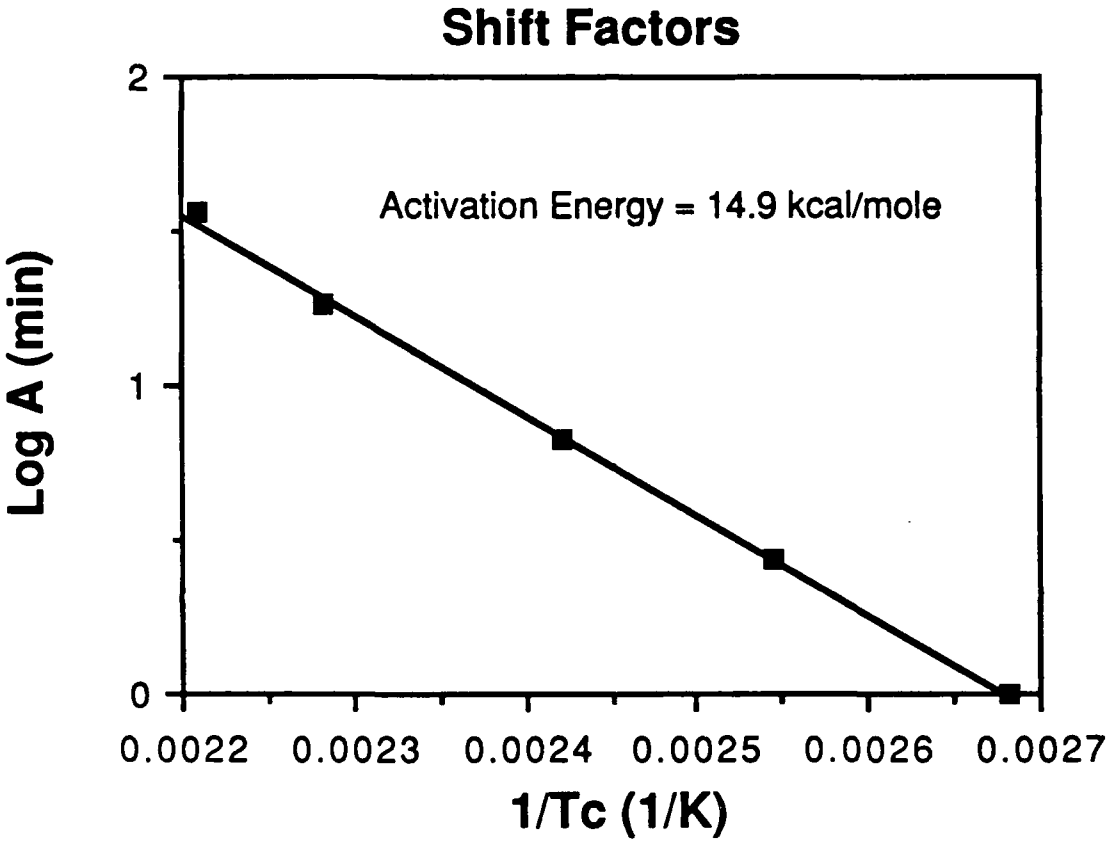
Shift Factors
Activation Energy = 14.9 kcal/mole
Log A (min)
2
1
0
0.0022
0.0023
0.0024
0.0025
0.0026
0.0027
1/Tc (1/K)

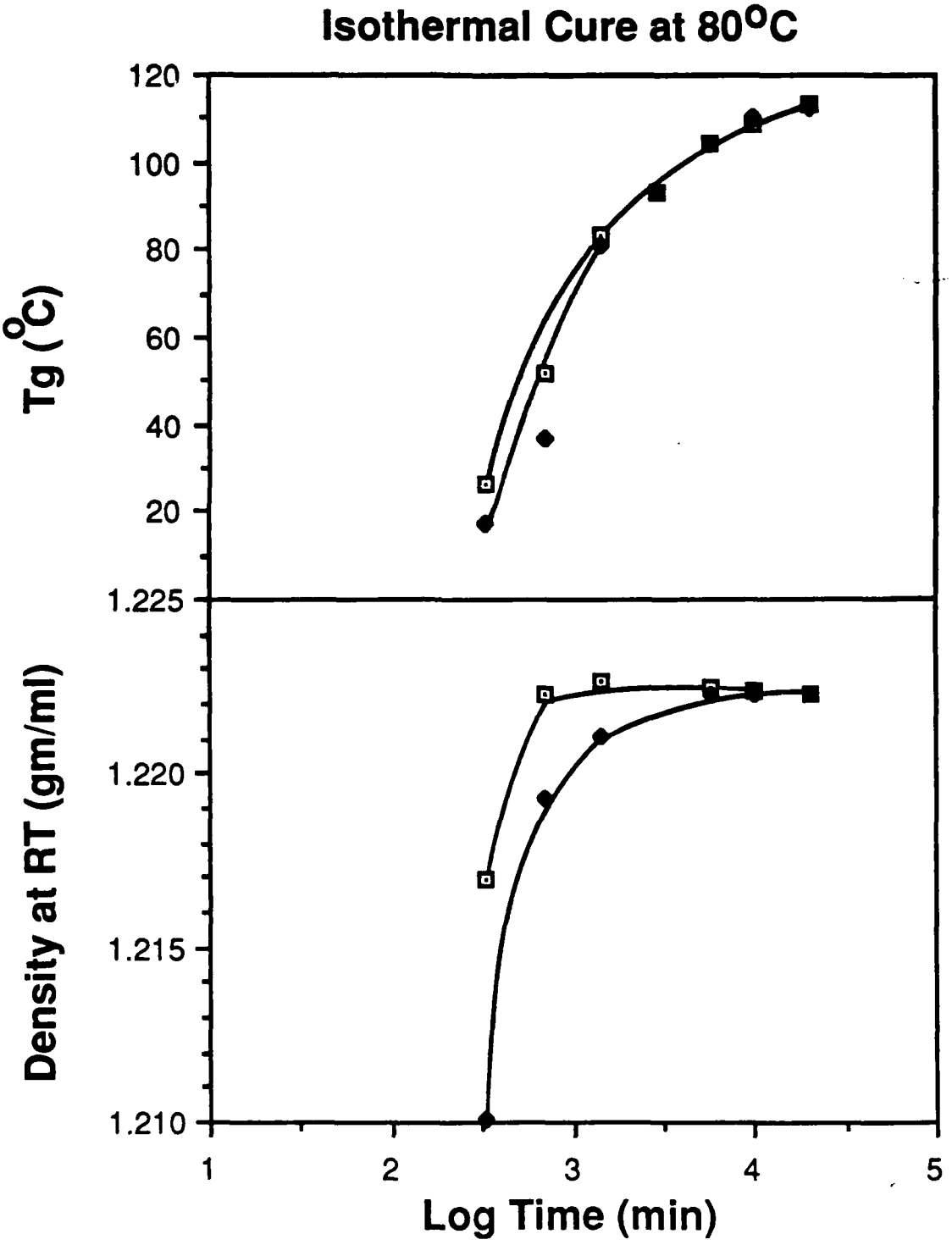
Isothermal Cure at 80°C
Tg (°C)
120
100
80
60
40
20
Density at RT (gm/ml)
1.225
1.220
1.215
1.210
1
2
3
4
5
Log Time (min)

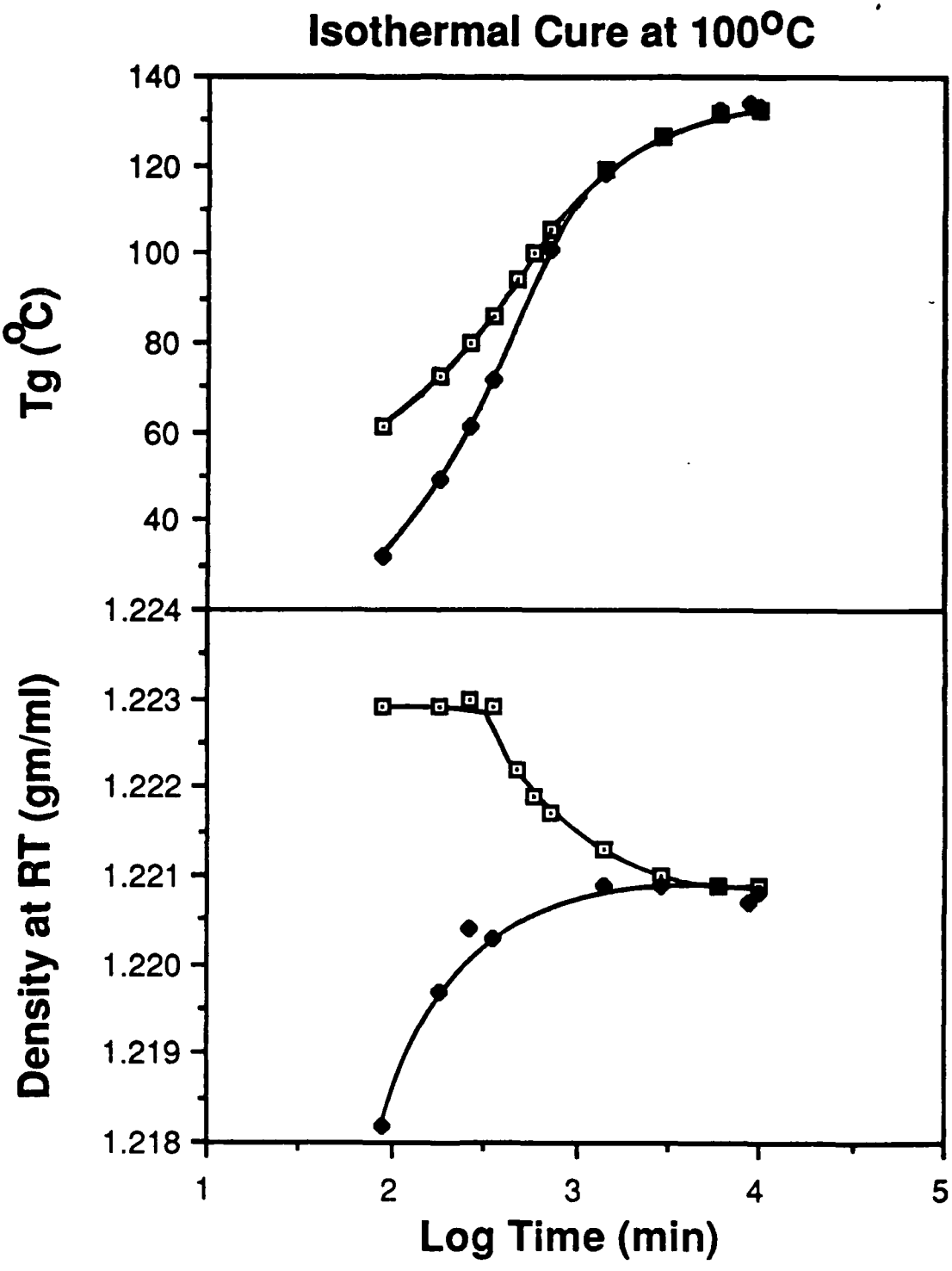
Isothermal Cure at 100°C
Tg (°C)
140
120
100
80
60
40
Density at RT (gm/ml)
1.224
1.223
1.222
1.221
1.220
1.219
1.218
1
2
3
4
5
Log Time (min)

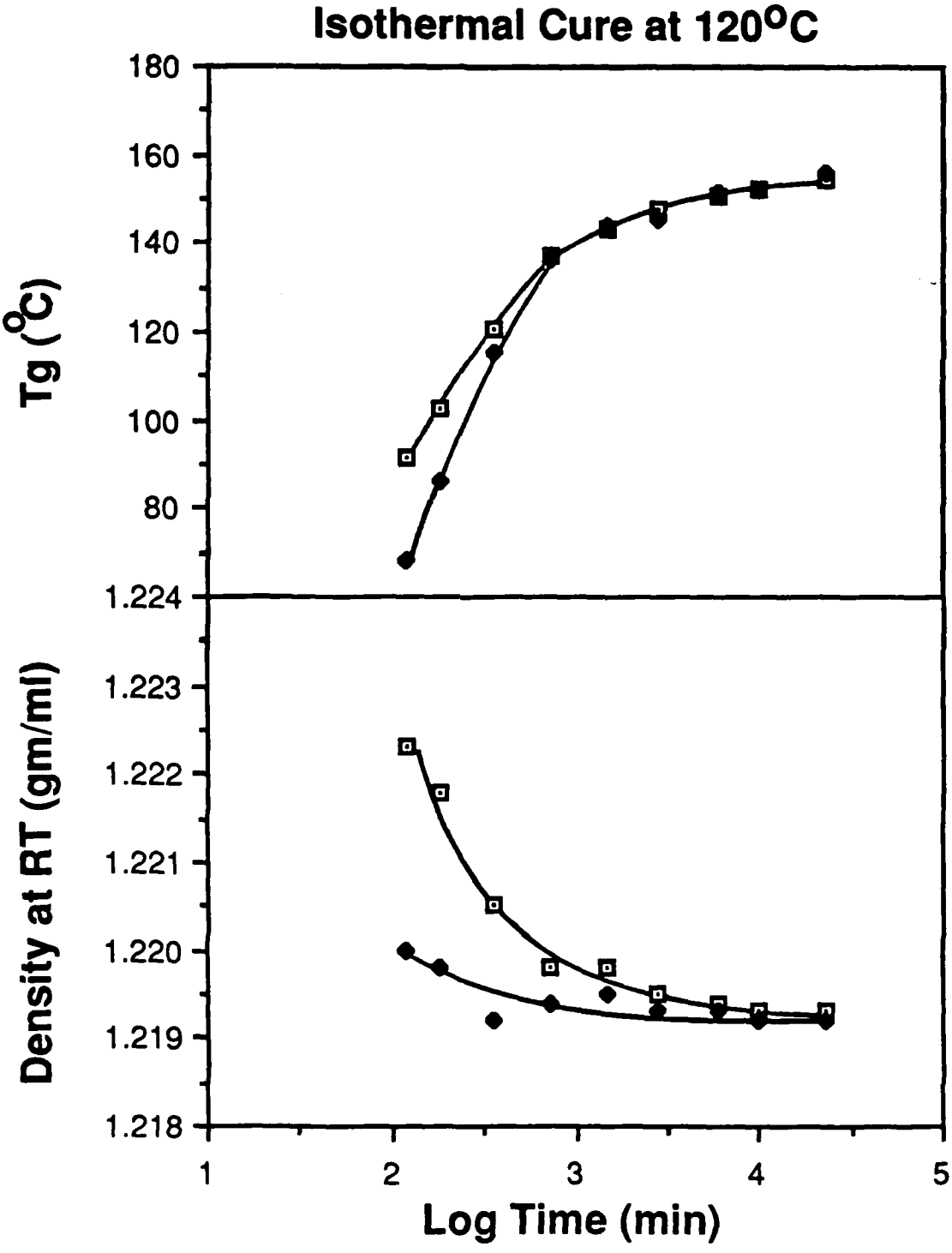
Isothermal Cure at 120°C
Tg (°C)
180
160
140
120
100
80
Density at RT (gm/ml)
1.224
1.223
1.222
1.221
1.220
1.219
1.218
1
2
3
4
5
Log Time (min)

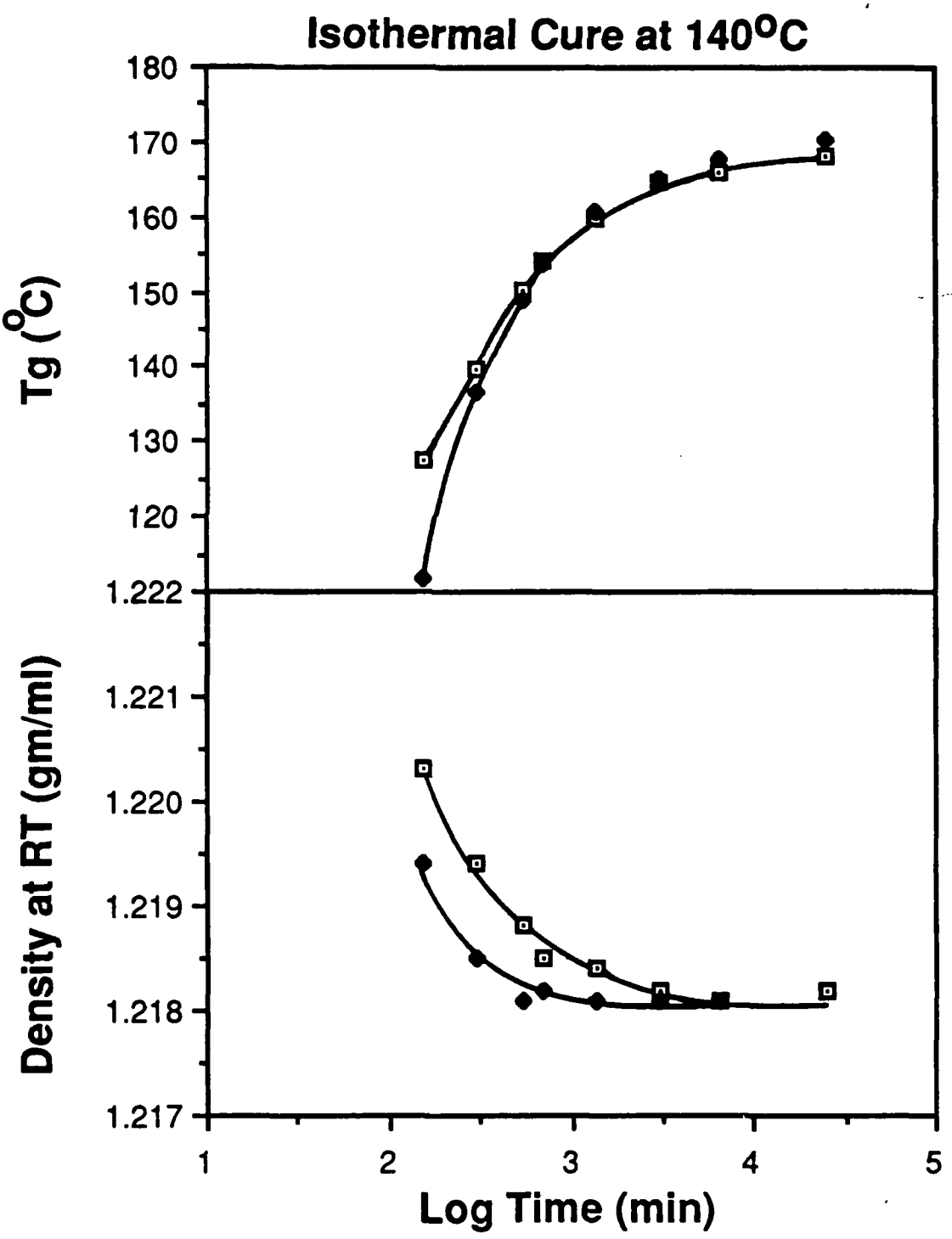
Isothermal Cure at 140°C
Tg (°C)
180
170
160
150
140
130
120
Density at RT (gm/ml)
1.222
1.221
1.220
1.219
1.218
1.217
1
2
3
4
5
Log Time (min)

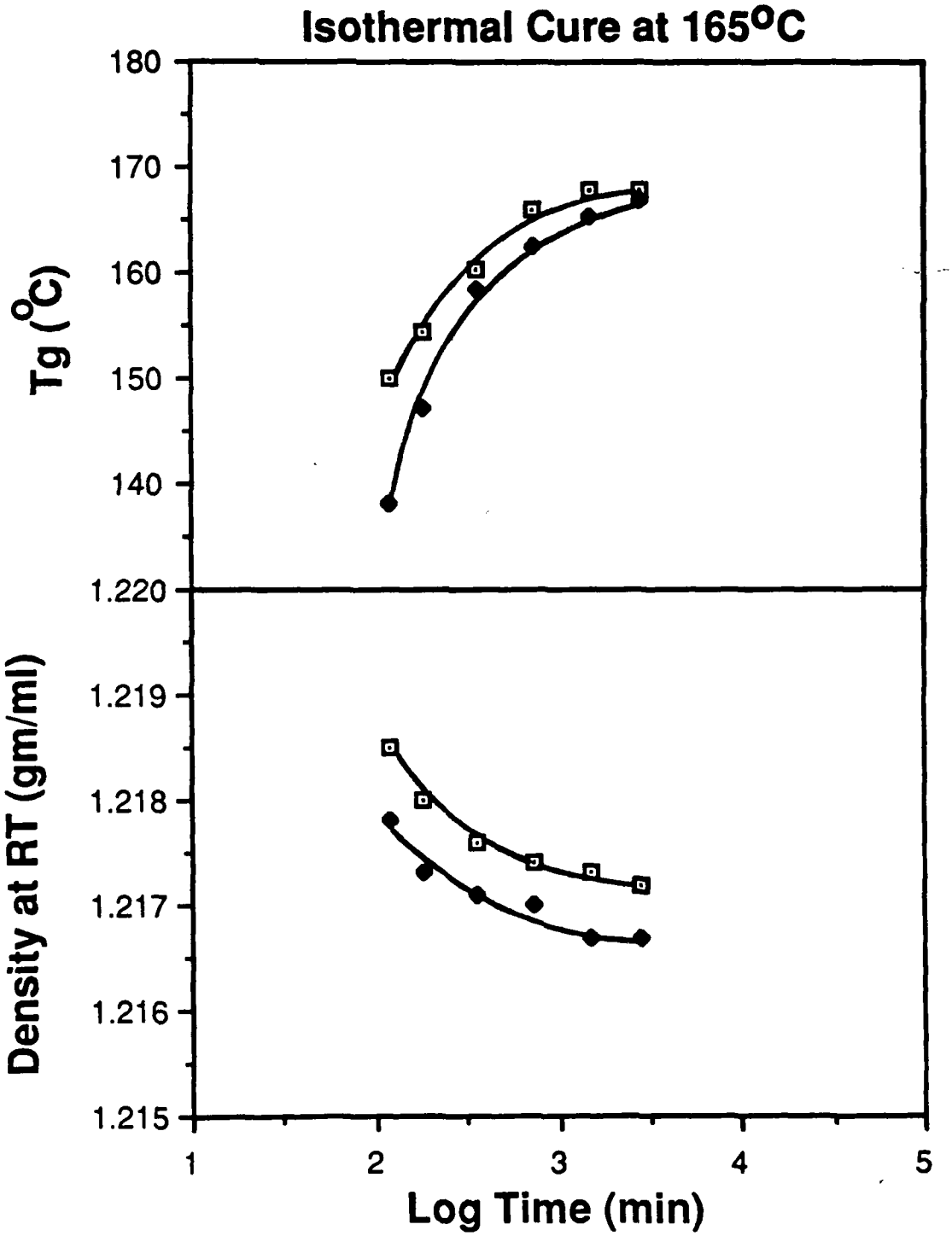
Isothermal Cure at 165°C
Tg (°C)
180
170
160
150
140
Density at RT (gm/ml)
1.220
1.219
1.218
1.217
1.216
1.215
1
2
3
4
5
Log Time (min)

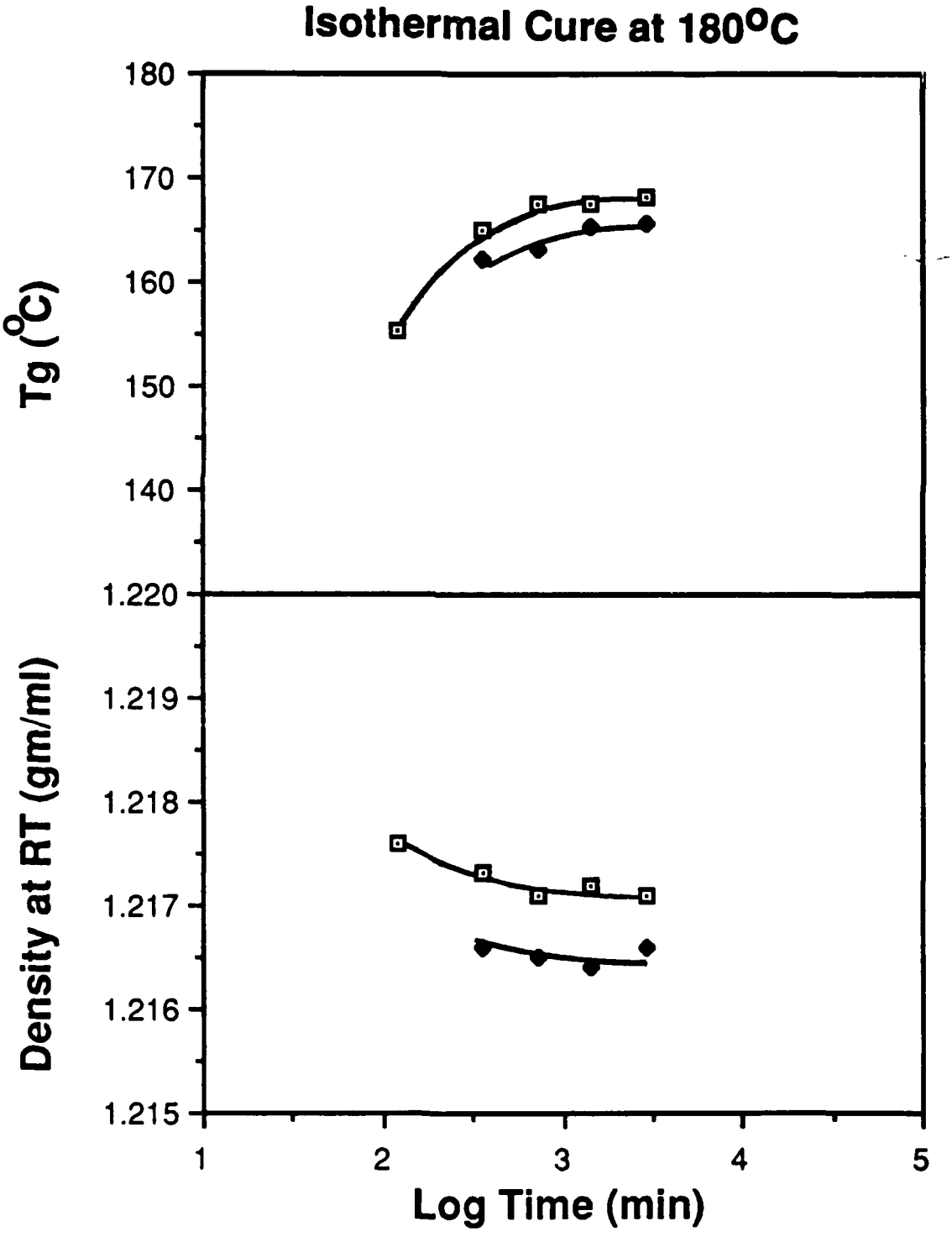
Isothermal Cure at 180°C
Tg (°C)
180
170
160
150
140
Density at RT (gm/ml)
1.220
1.219
1.218
1.217
1.216
1.215
1
2
3
4
5
Log Time (min)

Figure 10

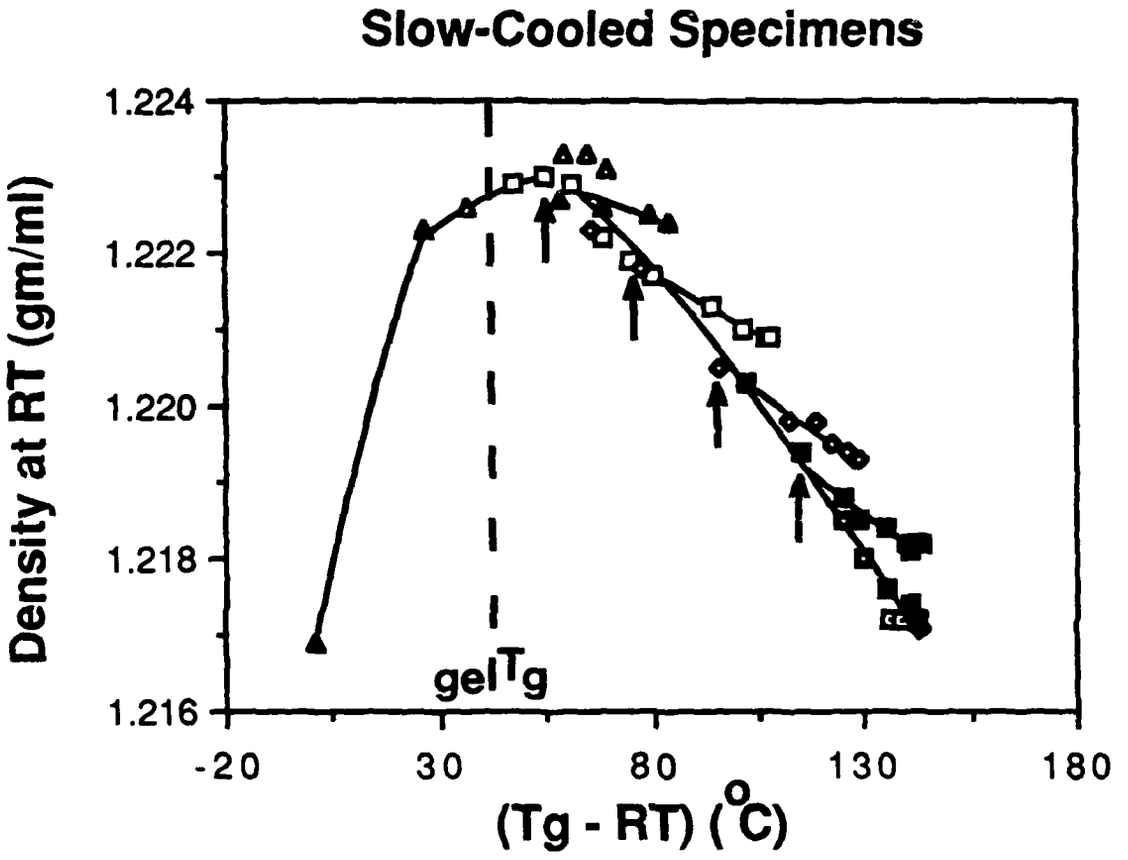
Slow-Cooled Specimens
Density at RT (gm/ml)
1.224
1.222
1.220
1.218
1.216
gel Tg
-20
30
80
130
180
(Tg - RT) (°C)

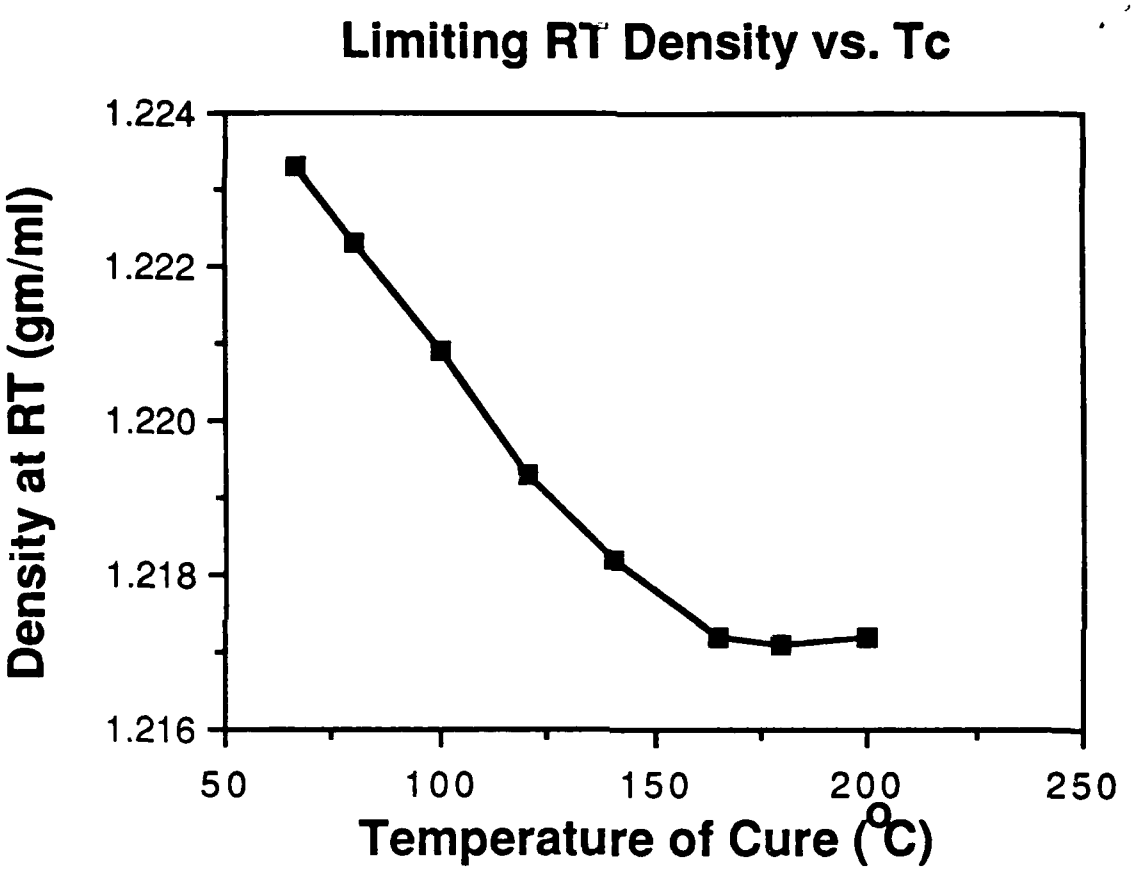
Limiting RT Density vs. Tc
Density at RT (gm/ml)
1.224
1.222
1.220
1.218
1.216
50
100
150
200
250
Temperature of Cure (°C)

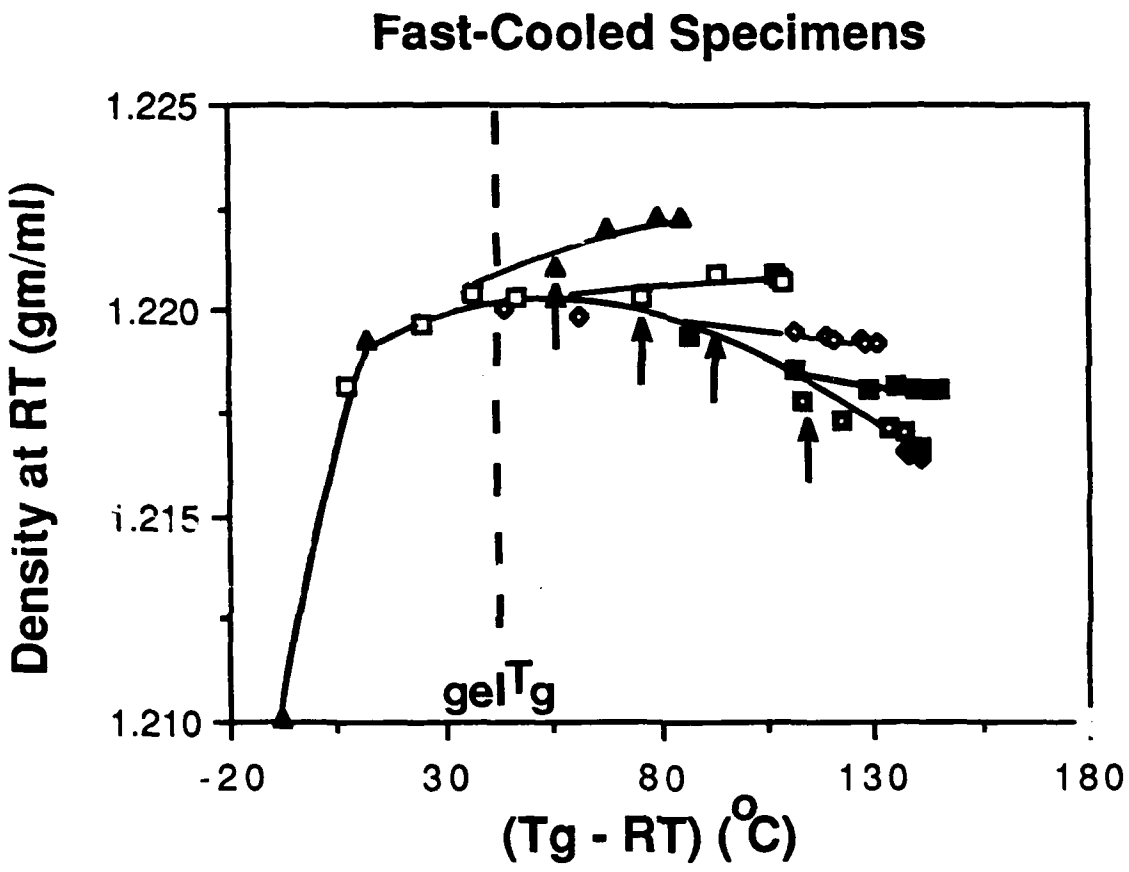
Fast-Cooled Specimens
Density at RT (gm/ml)
1.225
1.220
1.215
1.210
gel Tg
-20
30
80
130
180
(Tg - RT) (°C)

V-T Relationship of Amorphous Polymers

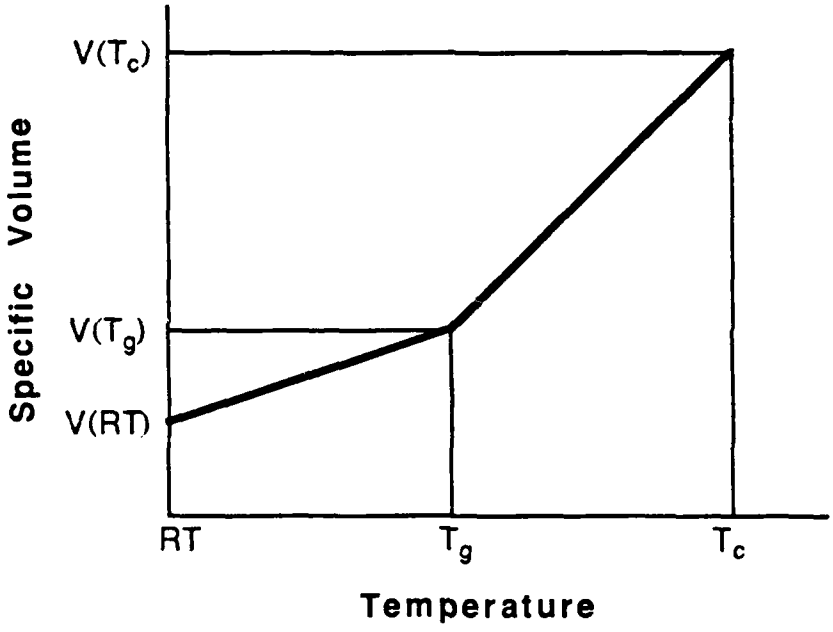

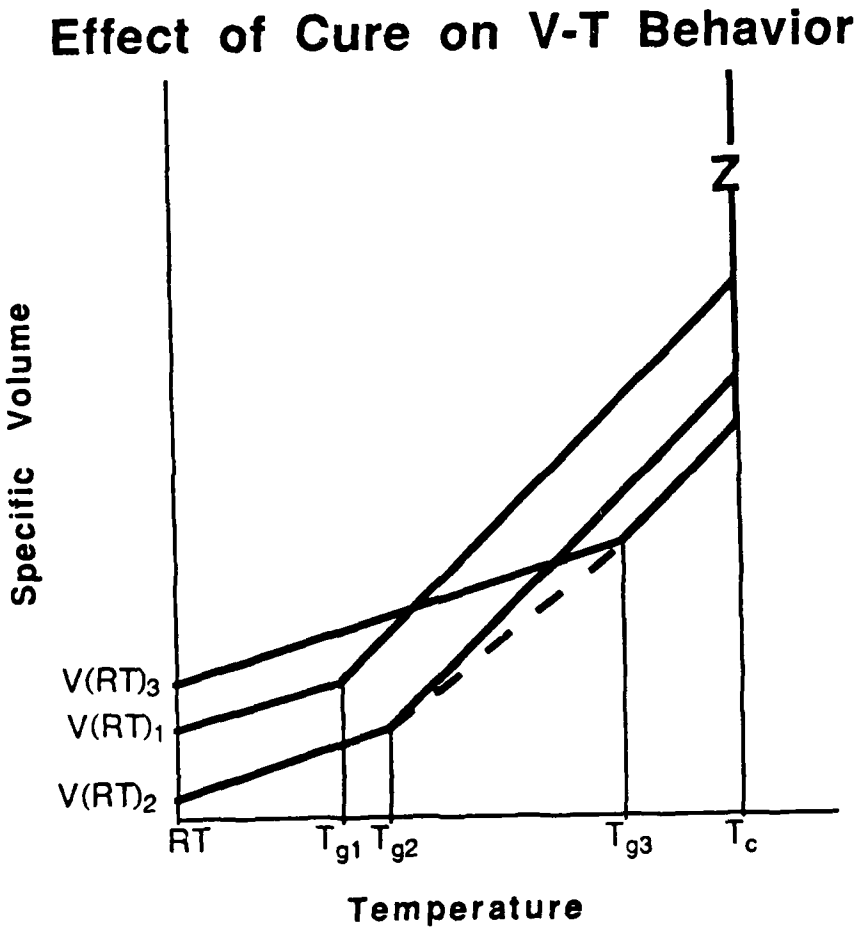
Effect of Cure on V-T Behavior
Z
Specific Volume
V(RT)3
V(RT)1
V(RT)2
RT
Tg1
Tg2
Tg3
Tc
Temperature

Figure 15

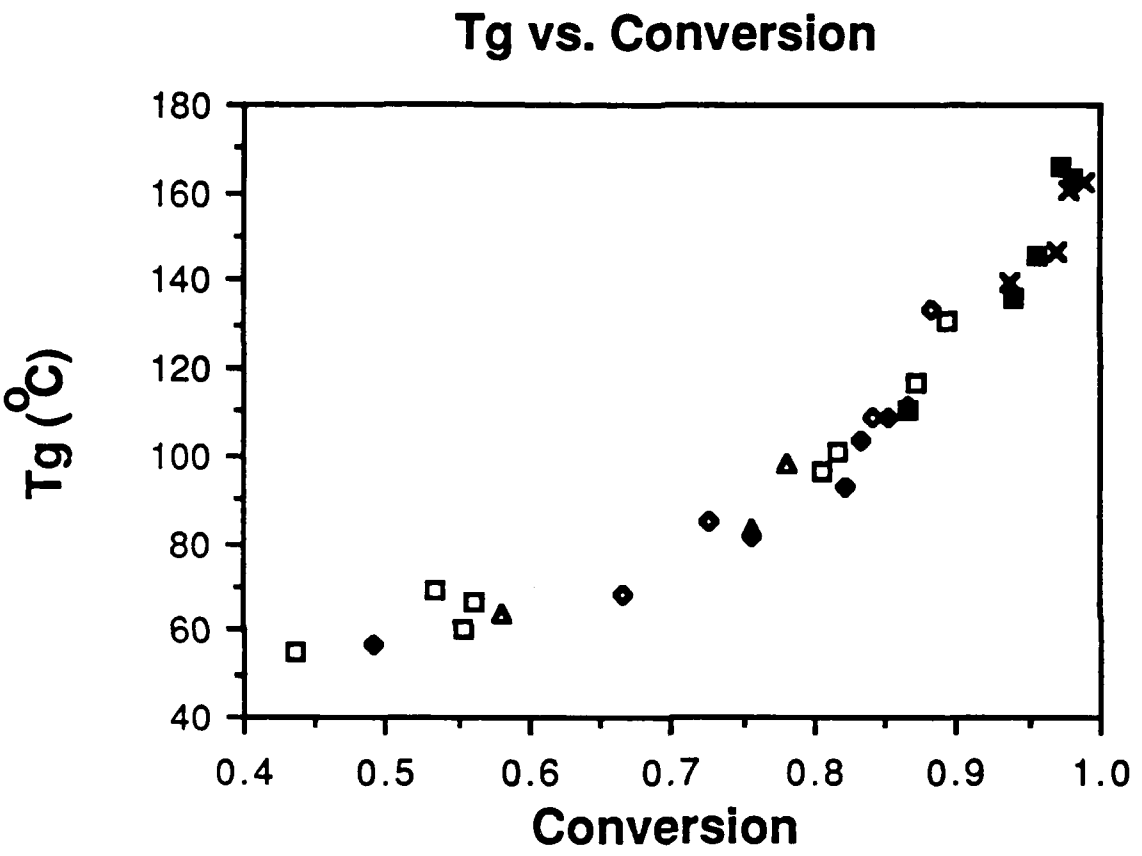
Tg vs. Conversion
Tg (°C)
180
160
140
120
100
80
60
40
0.4
0.5
0.6
0.7
0.8
0.9
1.0
Conversion

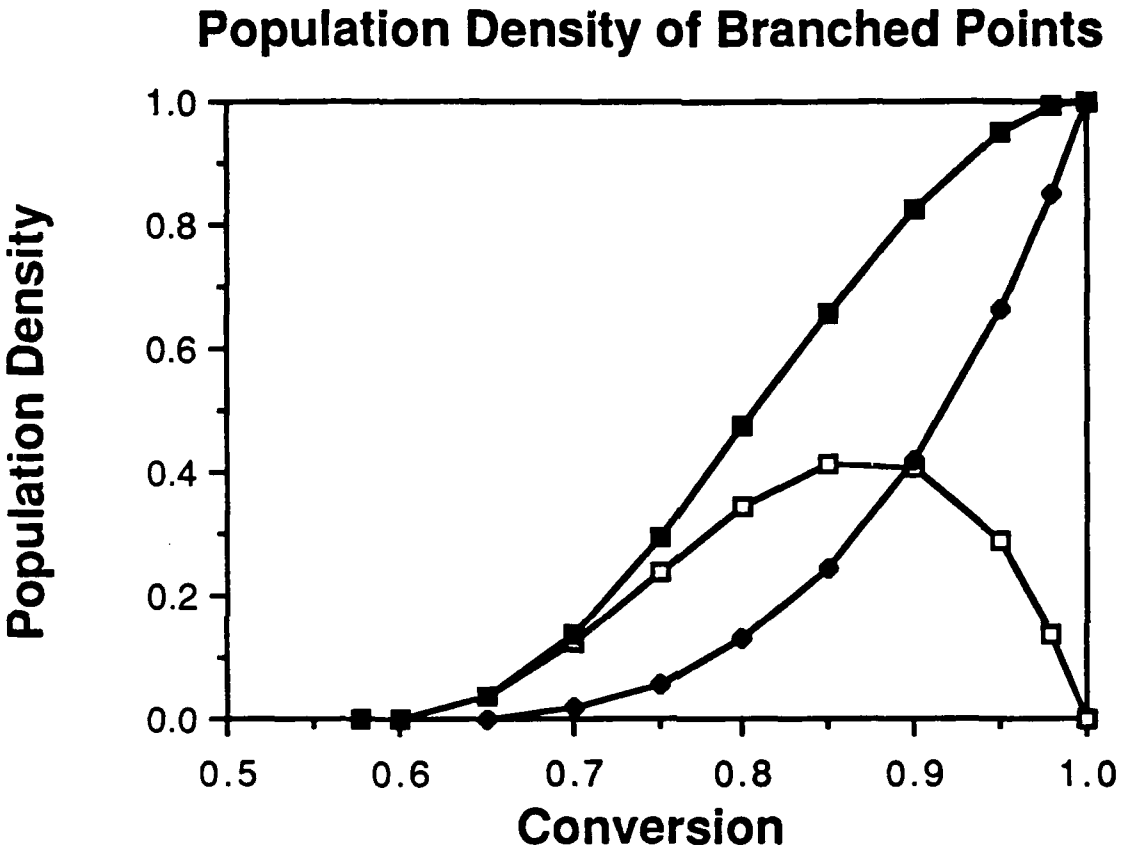
Population Density of Branched Points
Population Density
1.0
0.8
0.6
0.4
0.2
0.0
0.5
0.6
0.7
0.8
0.9
1.0
Conversion

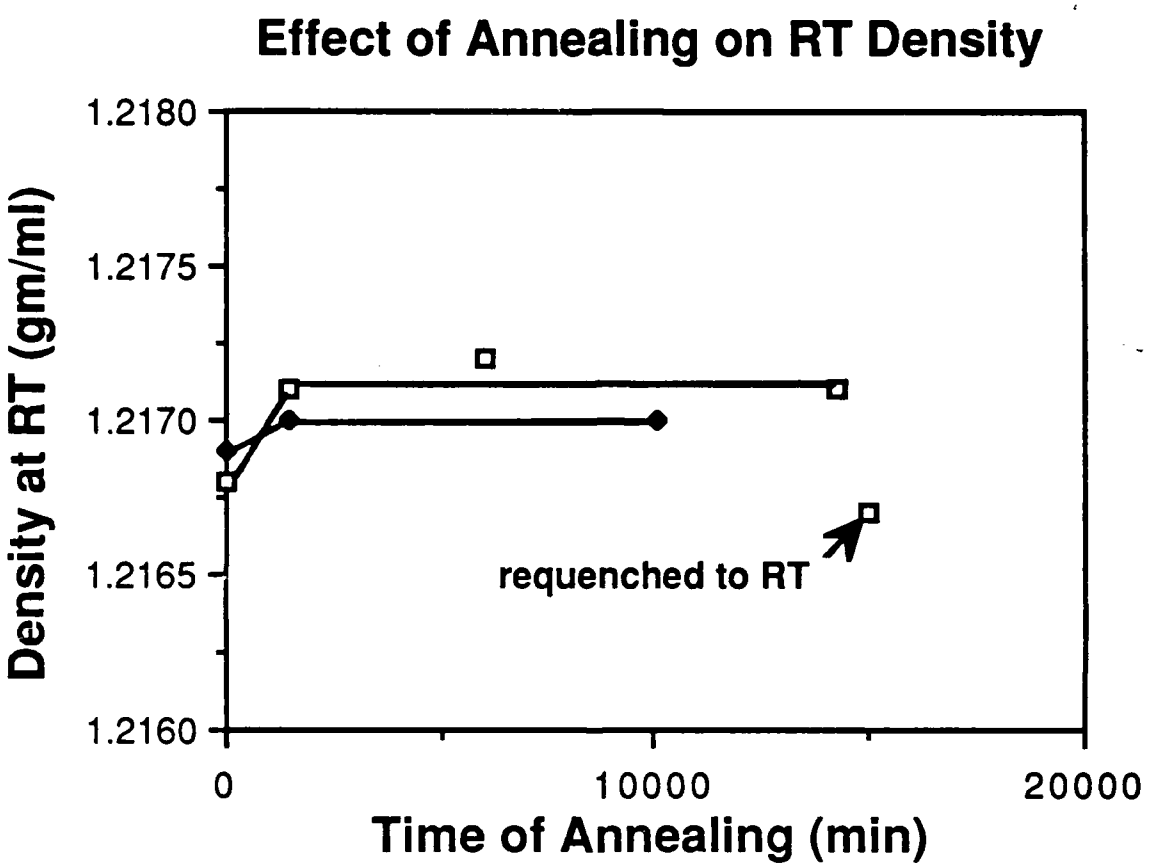
Effect of Annealing on RT Density
1.2180
1.2175
1.2170
1.2165
1.2160
Density at RT (gm/ml)
requenched to RT
0
10000
20000
Time of Annealing (min)

DL/1113/87/2

TECHNICAL REPORT DISTRIBUTION LIST, GEN

	No. Copies
Office of Naval Research Attn: Code 1113 800 N. Quincy Street Arlington, Virginia 22217-5000	2
Dr. Bernard Douda Naval Weapons Support Center Code 50C Crane, Indiana 47522-5050	1
Naval Civil Engineering Laboratory Attn: Dr. R. W. Drisko, Code L52 Port Hueneme, California 93401	1
Defense Technical Information Center Building 5, Cameron Station Alexandria, Virginia 22314	12 high quality
DTNSRDC Attn: Dr. H. Singerman Applied Chemistry Division Annapolis, Maryland 21401	1
Dr. William Tolles Superintendent Chemistry Division, Code 6100 Naval Research Laboratory Washington, D.C. 20375-5000	1
Dr. David Young Code 334 NORDA NSTL, Mississippi 39529	1
Naval Weapons Center Attn: Dr. Ron Atkins Chemistry Division China Lake, California 93555	1
Scientific Advisor Commandant of the Marine Corps Code RD-1 Washington, D.C. 20380	1
U.S. Army Research Office Attn: CRD-AA-IP P.O. Box 12211 Research Triangle Park, NC 27709	1
Mr. John Boyle Materials Branch Naval Ship Engineering Center Philadelphia, Pennsylvania 19112	1
Naval Ocean Systems Center Attn: Dr. S. Yamamoto Marine Sciences Division San Diego, California 91232	1